ADA042132

RADIOSCIENCE LABORATORY

STANFORD ELECTRONICS LABORATORIES
DEPARTMENT OF ELECTRICAL ENGINEERING
STANFORD UNIVERSITY · STANFORD, CA 94305

SEL-77-013

AIR/UNDERSEA COMMUNICATION AT ULTRA-LOW-FREQUENCIES USING AIRBORNE LOOP ANTENNAS

by

A. C. Fraser-Smith

D. M. Bubenik

O. G. Villard, Jr.

June 1977

TECHNICAL REPORT NO. 4207-6

DDC

JUL 27 1977

E

SEL-77-013

AD No.

DDC FILE COPY

UNCLASSIFIED

REPORT DOCUMENTATION PAGE		READ INSTRUCTIONS BEFORE COMPLETING FORM
1. REPORT NUMBER Tech. Report No. 4207-6	2. GOVT ACCESSION NO.	3. RECIPIENT'S CATALOG NUMBER
4. TITLE (and Subtitle) AIR/UNDERSEA COMMUNICATION AT ULTRA-LOW-FREQUENCIES USING AIRBORNE LOOP ANTENNAS		5. TYPE OF REPORT & PERIOD COVERED Technical January 1975-February 1977
		6. PERFORMING ORG. REPORT NUMBER SEL-77-013, TR-4207-6
7. AUTHOR(s) A. C. Fraser-Smith D. M. Bubenik O. G. Villard, Jr.		8. CONTRACT OR GRANT NUMBER(s) N00014-75-C-1095 ARPA Order No. 2494-1733
9. PERFORMING ORGANIZATION NAME AND ADDRESS Radioscience Laboratory, Stanford Electronics Laboratories, Stanford University, Stanford, CA 94305		10. PROGRAM ELEMENT, PROJECT, TASK AREA & WORK UNIT NUMBERS
11. CONTROLLING OFFICE NAME AND ADDRESS Defense Advanced Research Projects Agency Strategic Technology Office, 1400 Wilson Blvd., Arlington, VA 22209		12. REPORT DATE June 1977
		13. NUMBER OF PAGES 84
14. MONITORING AGENCY NAME & ADDRESS(if different from Controlling Office) Office of Naval Research Field Projects Programs, Code 461(FP) 800 North Quincy St., Arlington, VA 22217		15. SECURITY CLASS. (of this report) UNCLASSIFIED
		15a. DECLASSIFICATION/DOWNGRADING SCHEDULE

16. DISTRIBUTION STATEMENT (of this Report)

Approved for public release; distribution unlimited.

17. DISTRIBUTION STATEMENT (of the abstract entered in Block 20, if different from Report)

18. SUPPLEMENTARY NOTES

19. KEY WORDS (Continue on reverse side if necessary and identify by block number)

ULF, AIR/UNDERSEA COMMUNICATION, AIRBORNE LOOP ANTENNAS

20. ABSTRACT (Continue on reverse side if necessary and identify by block number)

In this report we investigate the possibility of using ultra-low-frequency (ULF) signals from airborne loop antennas (i.e., magnetic dipoles) for air/undersea communication. Because of the low data rate at ULF, communication is here understood to mean the transfer of short messages of high information content.

DD FORM 1473 EDITION OF 1 NOV 65 IS OBSOLETE
S/N 0102-LF-014-6601

UNCLASSIFIED

332 400

10 to the 7th ...

We use numerical integration to calculate the 1 Hz total magnetic field amplitudes in the sea at depths from 0 m to 200 m due to airborne unit moment vertical and horizontal magnetic dipoles at altitudes from 100 m to 10 km. Considering the magnetic moments m attainable with present aircraft power and payload capability ($m = 10^7$ Am^2 - 10^9 Am^2) and the minimum detectable amplitude for a 1 Hz signal beneath the sea (~ 1 mγ), we conclude that air/undersea communication at 1 Hz is possible under the following illustrative conditions: For a horizontal plane loop antenna at 3000 m altitude and a ULF receiver at a 100 m depth, communication is possible for horizontal distances to 10 km for $m = 10^7$ Am^2 and to 33 km for $m = 10^9$ Am^2. The corresponding limits for a vertical plane loop antenna are 13 km to 64 km. It is also possible, if desired, to limit communication to a comparatively small circular area directly beneath the aircraft. Sea floor effects can alter these values significantly, particularly if the receiver is near the floor.

m SUBGAMMA

IDtotheYih A&2'''

AIR/UNDERSEA COMMUNICATION AT ULTRA-LOW-FREQUENCIES
USING AIRBORNE LOOP ANTENNAS

by

A. C. Fraser-Smith

D. M. Bubenik

O. G. Villard, Jr.

Technical Report 4207-6

June 1977

ABSTRACT

In this report we investigate the possibility of using ultra-low-frequency (ULF) signals from airborne loop antennas (i.e., magnetic dipoles) for air/undersea communication. Because of the low data rate at ULF, communication is here understood to mean the transfer of short messages of high information content.

We use numerical integration to calculate the 1 Hz total magnetic field amplitudes in the sea at depths from 0 m to 200 m due to airborne unit moment vertical and horizontal magnetic dipoles at altitudes from 100 m to 10 km. Considering the magnetic moments m attainable with present aircraft power and payload capability ($m = 10^7$ A m^2 - 10^9 A m^2) and the minimum detectable amplitude for a 1 Hz signal beneath the sea (~ 1 mγ), we conclude that air/undersea communication at 1 Hz is possible under the following illustrative conditions: For a horizontal plane loop antenna at 3000 m altitude and a ULF receiver at a 100 m depth, communication is possible for horizontal distances to 10 km for $m = 10^7$ A m^2 and to 33 km for $m = 10^9$ A m^2. The corresponding limits for a vertical plane loop antenna are 13 km to 64 km. It is also possible, if desired, to limit communication to a comparatively small circular area directly beneath the aircraft. Sea floor effects can alter these values significantly, particularly if the receiver is near the floor.

Note: In this report we use ULF (ultra-low-frequencies)
       for frequencies less than 5 Hz. Pc 1 geomagnetic
       pulsations are observed in the upper part of this
       frequency range. ELF (extremely-low-frequencies)
       is used to designate frequencies in the range
       5 Hz to 3 kHz, VLF (very-low-frequencies) is used
       for frequencies in the range 3 - 30 kHz, and HF
       (high frequencies) is used for frequencies in the
       ranges 3 - 30 MHz.

CONTENTS

TABLES

ILLUSTRATIONS

I. INTRODUCTION

Submarines have long played an important role in national defense. In recent years, as the concept of deterrence has grown, the importance of ballistic-missile submarines has increased until they are now a primary element in the strategic-deterrent forces of both the U.S. and the U.S.S.R. (Scoville, 1972). Accompanying the increase in importance of submarines, there has been much technological innovation to ensure that the submarines can operate for long intervals at great depths. Because sea water is a conductor and attenuates electromagnetic waves, the increasing depth of operation of the submarines has increased the difficulty of communication between these vessels and their command centers. To help overcome this difficulty, the frequencies at which electromagnetic communication take place, or are planned to take place, have been steadily reduced.

Unlike ordinary high-frequency (HF; frequencies in the range 3 to 30 MHz) radio waves, which do not penetrate sea water to any distance, very-low-frequency (VLF; frequencies in the range 3 to 30 kHz) electromagnetic waves penetrate a short distance in sea water and a number of land-based VLF transmitting stations have been established at locations around the world for submarine communication. In addition, airborne VLF systems have been developed. To receive the VLF signals, a submarine operating at depth can trail an antenna close to the surface and thus reduce the attenuation of the signals produced by the sea water. However, it is obviously an inconvenience, and it may also be difficult or dangerous at times, to deploy these trailing antennas.

1

There has been much research on the use of extremely-low-frequency (ELF; frequencies in the range 5 Hz to 3 kHz) electromagnetic waves for submarine communication. The Sanguine project, for example, involved ELF waves with a carrier frequency of about 45 Hz (Wait, 1972). Because of their lower frequencies, these waves penetrate more effectively into sea water than VLF waves and they have other advantages, primarily propagation related, over VLF for communication (Bernstein et al., 1974). The data rate is low but apparently adequate for command communication purposes.

The use of ultra-low-frequency (ULF; frequencies less than 5 Hz) electromagnetic signals for undersea communication has received much less attention than the present or proposed uses of VLF and ELF waves. For world-wide strategic communication, proposed ground-based ULF antennas suffer from the same disadvantage as the ELF antennas: they have to be very large and require much power (e.g., Fraser-Smith et al., 1972; Greifinger, 1972; Davis, Willis, and Althouse, 1973; Greifinger and Greifinger, 1974; Davis and Willis, 1974; Harker, 1975). Furthermore, the ULF signals transfer data at a very low rate and they do not have all the desirable propagation characteristics of ELF waves. Nevertheless, ULF signals penetrate deeply in sea water with little loss (the skin depth for a 1 Hz electromagnetic wave in sea water is about 250 m) and for some purposes they may provide a useful undersea communication link.

In this report we make a preliminary assessment of the feasibility of using ULF signals from loop antennas (i.e., magnetic dipoles) to communicate down from an aircraft to a submerged receiver. This receiver may represent a submarine. However, manned submersibles, which are

being employed in increasing numbers for deep-sea and sea-bottom research (Arnold, 1967, Heirtzler and Grassle, 1976), and manned installations on the sea floor (possibly for mining), could also benefit from a low data rate communication channel. It is also possible that airborne ULF transmitters could be used for undersea search and rescue, just as low frequency electromagnetic techniques are being considered for use in mine rescue (Wait, 1971).

An obvious disadvantage of a communication system using frequencies in the ULF range is the low rate of data transfer, particularly in a military context where messages usually must be coded. It will therefore be impractical in almost all cases to send lengthy textual messages over a ULF communication link. However, such a link should be adequate for command and control messages, i.e., short messages of high information content. For example, it may be adequate merely to instruct a submerged receiver to rise closer to the surface where it could receive communications at higher frequencies. It is for this specific limited purpose of command and control that we believe ULF signals may be useful for air/undersea communication.

If there is to be an exchange of information between the aircraft and the submerged receiver it will probably also be necessary to have an undersea-to-air ULF communication channel in addition to the air-to-undersea channel. However, we believe the air/undersea channel is the most important and also the most difficult channel to establish. The difficulty arises because of limitations in the payload and electrical power capability of the transmitting vehicle. A practical ULF transmitter is likely to be heavy and require considerable power and we

3

consider the payload and power capability of an aircraft to be more limited than the same capability of a submerged ULF transmitting vehicle. Since this is basically a feasibility study, we consider only the more limited air/undersea ULF communication channel in this report.

In outline, the report consists of the following: (a) a chapter containing a brief discussion of the theoretical expressions for the ULF magnetic fields produced in the sea by ULF magnetic dipole sources located above the sea, and describing our numerical integration technique for obtaining these fields, (b) a chapter presenting the results obtained by numerical integration for the total magnetic field produced in the sea (for depths in the range 0 to 200 m) by unit moment ULF magnetic dipoles (frequency 1 Hz) at a range of elevations above the sea (elevations in the range 100 m to 10 km), (c) a chapter containing a discussion of the payload and power capability of a P-3 Orion aircraft, which we will take to be our standard, and derivation of a possible range of magnetic moments for an airborne loop antenna, (d) a final chapter where we combine the results of (b) and (c) to derive the ranges over which air/ undersea communication should be possible and where we discuss the feasibility of the method of communication. Because measurements of the total magnetic field can be omnidirectional (unlike measurements of a component of the magnetic field), and an omnidirectional receiving capability is likely to be a requirement for an air/undersea communication system, the calculations and discussion in this study are restricted to the total magnetic field produced in the sea by elevated ULF magnetic dipole sources.

4

We also report the results of several subsidiary studies that
are relevant to the feasibility study or to air/undersea communication
at ULF and ELF in general. For example, we investigate the relevance of
the concept of skin depth at ULF, where the points at which the fields
are evaluated are often much less than a wavelength away from the
source, and we show that the skin depth still provides a good indication
of the attenuation of ULF fields as they penetrate sea water. We also
investigate the range of validity of the approximate formulas given by
Kraichman (1970) for the field generated in the sea by dipoles above the
surface. For the case of a vertical magnetic dipole we calculate the
effect of a sea floor on the fields produced in the sea and, finally,
for a very deep sea and a 1 Hz frequency, we calculate the impedance
changes produced in the airborne current loop by the presence of the sea.

II. METHOD OF CALCULATION OF THE UNDERSEA FIELDS

The electromagnetic field expressions relevant to the problem of communication between an airborne loop antenna and a submerged receiver have been known for some time. Their development can be traced to the pioneering work of Sommerfeld (1909). The expressions involve complex integrals (often referred to as Sommerfeld integrals), which are difficult and often impossible to evaluate analytically. Thus, until the comparatively recent development of fast and accurate methods of numerical integration using digital computers, progress in evaluating the electromagnetic field expressions for air/undersea communication has been severely restricted. An important contribution was made by Durrani (1962, 1964), who derived simplified but necessarily approximate expressions for the undersea electromagnetic fields produced by airborne electric and magnetic dipoles. Additional expressions are collected in handbook form by Kraichman (1970). However, as we will show, these expressions are not always adequate for consideration of air/undersea communication at frequencies in the ULF range: they fail at short source-receiver distances and are of uncertain accuracy at intermediate distances. In this report we present the results of field calculations using a numerical integration technique. These results are of great accuracy and apply at all frequencies and source-receiver distance at which the quasistatic approximation is valid.

In this chapter we will first present the integral expressions for the magnetic fields produced in the air by airborne vertical and horizontal magnetic dipoles (corresponding to airborne horizontal and vertical loop antennas, respectively). We will then briefly review the

7
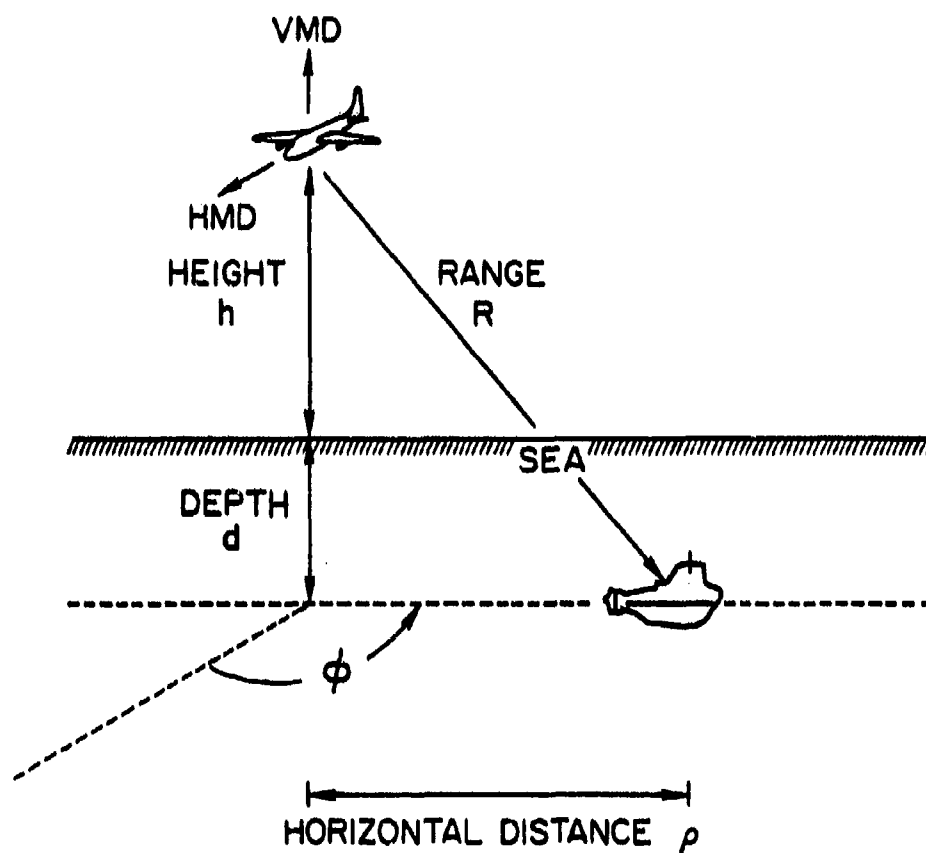
Figure II-1. Geometry for air/undersea communication.

previous work on the approximate analytical evaluation of these expressions. Finally, we will describe our numerical integration technique for evaluating the field expressions.

1. The Field Expressions

The geometry used in formulating the field expressions is shown in Figure II-1. We use a cylindrical coordinate system (ρ, ϕ, z), in which the sea (of conductivity $\sigma_s = 4$ mho/m) occupies the half-space $z \leq 0$, and the complementary region $z > 0$ is free space $(\sigma = 0)$. In certain cases, a sea floor $(\sigma = \sigma_g)$ will be allowed to occupy the region $z \leq -D$ otherwise the sea will be considered to be of infinite depth $(D \to \infty)$. The transmitter is modeled as a harmonic magnetic dipole of moment $me^{i\omega t}$ located at $(h, 0, 0)$. We shall justify the choice of a magnetic dipole shortly on the basis of the work of Durrani (1964). Two dipole orientations will be treated: a vertical magnetic dipole (VMD) pointing in the $+z$ direction, and a horizontal magnetic dipole (HMD) oriented along $\phi = 0$. The dipole approximation is valid provided the distance R from the source to the receiver (located at $\rho, -d, \phi$) is much greater than the characteristic dimension of the actual transmitter antenna. The expressions for the VMD were adapted from the work of Ryu et al. (1970), whose formulation permits the computation of the subsurface fields in a layered conducting medium (i.e., the effects of the sea floor may be examined), and also includes loop antennas of finite radius (which permits the straightforward computation of the antenna input impedance). The expressions for the HMD were taken from the work of Baños (1966), who developed a unified treatment of the fields of ideal dipole sources in the vicinity of a homogeneous conducting half space.

9

The field expressions used in this work are

$$B_\rho(\text{VMD}) = \frac{\mu_o m}{2\pi} \int_0^\infty g_1(\lambda)\, u_s\, [u_g + u_s\, \tanh u_s d']\, J_1(\lambda\rho)\, d\lambda \qquad (\text{II-1})$$

$$B(\text{VMD}) \equiv 0 \qquad (\text{II-2})$$

$$B_z(\text{VMD}) = \frac{\mu_o m}{2\pi} \int_0^\infty g_1(\lambda)\, \lambda\, [u_s + u_g\, \tanh u_s d']\, J_0(\lambda\rho)\, d\lambda \qquad (\text{II-3})$$

$$B_\rho(\text{HMD}) = \frac{\mu_o m}{2\pi}\, \cos\phi \int_0^\infty u_s\, g_2(\lambda)\, \left| \frac{1}{\lambda\rho} J_1(\lambda\rho) - J_0(\lambda\rho)\ d\lambda \right| \qquad (\text{II-4})$$

$$B_\phi(\text{HMD}) = \frac{\mu_o m}{2\pi}\, \sin\phi \int_0^\infty u_s\, g_2(\lambda)\, \left| \frac{1}{\lambda\rho} J_1(\lambda\rho) \right|\, d\lambda \qquad (\text{II-5})$$

$$B_z(\text{HMD}) = -\frac{\mu_o m}{2\pi}\, \cos\phi \int_0^\infty \lambda\, g_2(\lambda)\, J_1(\lambda\rho)\, d\lambda \qquad (\text{II-6})$$

where

$$g_1(\lambda) = \frac{\lambda^2\, [1 + \tanh u_s D]\, e^{-(\lambda h + u_s d)}}{[1 + \tanh u_s d']\, [u_s\, (u_g + \lambda) + (u_s^2 + \lambda u_g)\, \tanh u_s D]}$$

$$g_2(\lambda) = \frac{\lambda^2 e^{-(\lambda h + u_s d)}}{u_s + \lambda}$$

$$u_s^2 = \lambda^2 + i\omega\mu_o\sigma_s$$

$$u_g^2 = \lambda^2 + i\omega\mu_o\sigma_g$$

$$d' = D - d$$

10

These expressions are for the quasistatic case, that is, all displacement currents are neglected. This is permissible since, for all frequencies ω and slant ranges R to be considered here, $\omega R/c \ll 1$, where c is the velocity of light. Equations (1) through (3) include a sea bottom of conductivity σ_g at depth D. The corresponding formulas for an infinitely deep ocean are obtained by setting $d = D = \infty$ or $u_g = u_s$.

2. Review of Earlier Work

Most previous studies of air/subsurface communication links have been carried out using asymptotic expansions of the integrals (II-1) - (II-6), subject to simplifying assumptions. The most extensive published analysis is that of Durrani (1962, 1964), who considers undersea communication using magnetic dipoles, and derives simplified expressions for the electromagnetic fields produced in the sea (which is considered to be infinitely deep) by airborne vertical and horizontal dipoles. However, these expressions are valid only in the "quasi-near" range, which moves away from the dipole source as the frequency decreases. Durrani restricts his analysis to frequencies in the range 10 Hz to 100 kHz, and thus does not consider ULF frequencies. At 10 Hz, he calculates the "quasi-near" range to be 56.2 m to 4780 km, and estimates his results to be correct to within 0.5% for distances in the range 562 m to 478 km. For a frequency of 1 Hz, which we take to be our representative ULF frequency, the minimum source-receiver distance R for the "quasi-near" approximation to be valid is $\sqrt{10}$ times larger than at 10 Hz, i.e., the minimum distance for less than 0.5% error is about 1.8 km. However, values of R much less than 1.8 km could well be important for air/

11

undersea communication at ULF and thus the simplified expressions used by Durrani are not adequate for this study.

In the earlier analysis, Durrani (1962) derived simplified expressions for the electromagnetic fields produced in the sea by electric dipoles located above the sea. In his later work (Durrani 1964), he compares the magnetic dipole results with those for the electric dipole and concludes that the magnetic dipole is more effective in most cases for air/undersea communication. Although his results are not directly applicable to the ULF range, the lowest frequency considered by Durrani is probably close enough to the ULF range for his conclusion about the magnetic dipole to be valid at ULF. Thus, in considering the feasibility of air/undersea communication at ULF, we have considered a magnetic loop antenna instead of a trailing wire or other form of electric dipole. Other work by the authors, to be reported later, verifies that the magnetic loop is superior to the electric dipole for air/undersea communication at ULF.

To obtain a complete specification of the fields over the entire range of ρ, h, d, and ω, it is necessary to integrate (II-1) - (II-6) numerically. A numerical study of the subsurface fields of a horizontal loop antenna (VMD) located at and above the surface of a homogeneous conducting medium has been published by Wait and Spies (1972), who considered the problem of communicating with trapped miners. However, although they evaluated the complete field expressions for a wide range of frequency and conductivity, their results do not cover the complete range of parameters of interest in air/undersea communications at ULF, and also their results are presented using a form of normalized variables which is not easily interpreted.

The studies cited above neglect the effect of the ocean floor. As will be shown later in this report, this neglect is justified if the floor is more than about 1 skin depth below the receiver, but the bottom effects become quite pronounced when the receiver and the bottom are in closer proximity. Although approximate formulas are given in Kraichman (1970) for the fields in the presence of the ocean floor, they are useful only at very great distances from the source. To the authors' knowledge, the present study is the first to treat bottom effects in a complete fashion and over the entire range of source-receiver distances.

In summary, we have found that neither the approximate analytical approach to the evaluation of the field expressions nor the numerical integration approach have been applied to the problem of air/undersea communication at ULF. We have therefore applied our previously-developed numerical integration technique to this new situation. Details of the technique are given in the following section; a more complete description is given by Bubenik (1977).

3. Evaluation of the Field Expressions

Two different techniques were employed in the numerical integration of the field expressions (II-1) - (II-6). The primary, simpler method used Guass-Laguerre quadrature rules to reduce the integrals to straight-forward summations, as shown below.

$$\int_0^\infty f(\alpha) \, e^{-\alpha} \, d\alpha = \sum_{i=1}^N w_i \, f(\alpha_i)$$

Here, w_i and α_i are the set of weights and abscissas computed with respect to the weight function $e^{-\alpha}$ for quadrature rules with $N = 2, 4, 8, \cdots 256$. These quadrature rules were applied to each integral in order

13

of increasing N until the results of two successive applications
agreed to within a relative error limit of 10^{-4}. The weights and
abscissas were themselves computed using a fast numerical technique
recently developed at Stanford University by Golub and Welsch (1969)
which, unlike previous methods, does not explicitly require the roots
of the Laguerre polynomials to be found.

The Gauss-Laguerre technique works very well whenever $\rho/(h+d) < 2$.
Beyond this limit, the order N required exceeds 256 and increases
rapidly as this ratio increases, making this technique impractical at
very large horizontal distances. Often, the approximate formulas given
by Kraichman (1970) are useful in this case; but it sometimes happens,
particularly when the effects of the ocean bottom are considered, that
there exists a regime where neither the Gauss-Laguerre technique nor the
approximate formulas are useful. A second integration method was there-
fore developed.

The numerical integration strategy exploits the oscillatory nature
of the integrands in equations II-1 through II-6, which arises because
of the presence of the Bessel functions J_0 and J_1. Both the real and
the imaginary parts of the integrands have this general oscillatory form.
In outline, we integrate in sequence over the positive and negative half-
cycles of $f(\lambda)$ until the contribution A_i from the last of these sub-
integrations is less than a specified error bound. In theory, this
procedure will always work; however, to implement it in a straight-
forward manner is very inefficient as the envelope of $f(\lambda)$ is only
weakly damped as $\lambda \rightarrow \infty$, particularly for small values of h and d.
A more efficient scheme is to form a converging sequence of partial sums

14

approximating the integral by adding the results of successive half-cycle integrations to each previous subtotal, and then to apply an appropriate transformation to accelerate the convergence of this sequence.

The sequence formed by adding the terms of alternating signs derived from the half-cycle sub-integrations is well suited to the e_m nonlinear sequence-sequence transform described by Shanks (1955), and we therefore implemented this transform. The sub-integrals A_i were computed using Romberg adaptive quadrature. The Romberg integrations were carried out to a relative accuracy of 10^{-5}, and the relative error bound for each complete integral was set at 10^{-4}. All computations were performed in double precision arithmetic on an IBM 370/168 machine.

The Romberg-Shanks procedure was found to fill effectively the gap between the Gauss-Laguerre technique and the approximate formulas. It is useful even at very large values of $\rho/(d + h)$. However, it becomes extremely inefficient at small values (<1) of this ratio. The two methods are therefore complementary; with the Romberg-Shanks technique taking over from Gauss-Laguerre as $\rho/(d + h)$ increases beyond a value of about 2 (Bubenik, 1977).

15

II. RESULTS OF CALCULATIONS

In this chapter we present the magnetic field data obtained by
numerical integration for the VMD and the HMD at the representative
ULF frequency of 1 Hz. The data were calculated for unit moment dipoles
and for a dipole of arbitrary moment the field values should be multi-
plied by the dipole moment to obtain the corresponding field amplitudes.
We use the milligamma (1 mγ = 10^{-12} Tesla) as our unit for the magnetic
field. The purpose of Section 1 is to show that the attenuation in sea
water of the electromagnetic fields from an elevated harmonic dipole can
be usefully estimated by using a skin depth approach. In Section 2 and
3 we present the major portion of our calculated magnetic field data
for the VMD and HMD, and these data are compared in Section 4. Further
results relevant to the applicability of Kraichman's (1970) approximate
analytical expressions, and the effects produced by a sea floor, are
given in Sections 5 and 6. Finally, in Section 7 we present data illus-
trating the impedance changes produced by the sea in an airborne current
loop.

1. Verification of the Skin Depth Approximation

The skin depth at angular frequency ω for an electrically con-
ducting but non-magnetic material (permeability μ_0) of conductivity σ
is defined by the equation

$$\delta = \sqrt{\frac{2}{\omega\mu_0\sigma}} \qquad\qquad (III-1)$$

This equation is typically derived by considering a plane electromagnetic
wave of angular frequency ω falling normally onto the plane surface of
the conducting material. It is found that the amplitudes of the fields

17

decrease exponentially with depth as $e^{-d/\delta}$, and thus δ is the depth at which the electric and magnetic fields fall to 1/e of their values just inside the surface.

The skin depth is a convenient and useful parameter for characterizing the attenuating properties of a particular conducting material. However, it is not certain that the electromagnetic fields from a dipole source close to the surface of a conducting material will exhibit an $e^{-d/\delta}$ dependence on depth. The reason for the possible discrepancy is that, if the source is close to the conducting material (or more specifically, less than a wavelength away), the electromagnetic fields do not reach the surface in the form of a plane wave. In addition to wavefront curvature, the fields will also have a significant induction (or near) field component, which decays more rapidly with distance than the radiation field component.

At ULF and in the lower part of the ELF range the wavelengths of electromagnetic waves in free space are very large. For example, the wavelength of a 7.5 Hz wave is comparable to the circumference of the earth, and at 100 Hz the wavelength is still large at 30,000 km. Thus, in considering air/undersea communication at frequencies less than 100 Hz, the source and receiver are likely to be separated by much less than one wavelength. The question then arises: do the ULF/ELF electromagnetic fields produced in sea water by an airborne magnetic dipole source fall off as $e^{-d/\delta}$ below the sea surface?

To answer this question, we calculated the amplitudes of the total magnetic field produced at depths in the range $0 \leq d \leq 300$ m, and at a horizontal distance of $\rho = 1.0$ km in an infinitely deep sea, by unit moment horizontal and vertical magnetic dipoles located at an altitude

18

of h = 300 m. We considered the two frequencies 1.0 Hz and 45.0 Hz, and the results of our calculations are presented in Figures. III-1 and III-2.

Figure III-1 shows the 1.0 Hz and 45.0 Hz total magnetic fields produced by the VMD. The scales in both this figure and Figure III-2 were chosen to provide a straight line representation for an exponentially declining total field, i.e., the depth scale is linear, whereas the total magnetic field scale is logarithmic. The actual calculated total fields are given by the solid lines which are straight, indicating exponential fall off with depth. The broken lines show the $e^{-d/\delta}$ fall off that would occur if the skin depth concept completely characterized the field variation. As can be seen in the Figure, the two sets of lines are close but do not coincide. Figure III-1 also emphasizes the great difference between 1 Hz and 45 Hz electromagnetic signals in their ability to penetrate sea water. The amplitudes of the 1 Hz and 45 Hz signals are nearly the same just beneath the sea surface, but at a depth of 300 m the amplitude of the 45 Hz signal is reduced more than three orders of magnitude below the amplitude of the 1 Hz signal.

Figure III-2 shows the 1.0 Hz and 45.0 Hz total magnetic fields produced by the HMD for the two azimuthal angles $\phi = 0°$ and $\phi = 90°$. The same conclusions as for the VMD apply: the total fields fall off exponentially at a rate approximately characterized by the skin depth and there is much greater attenuation at 45.0 Hz than at 1.0 Hz.

Although the results presented in Figures III-1 and III-2 cover only selected frequencies in the ULF and ELF ranges, and a limited range of possible receiver depths, source heights, or source-receiver

19
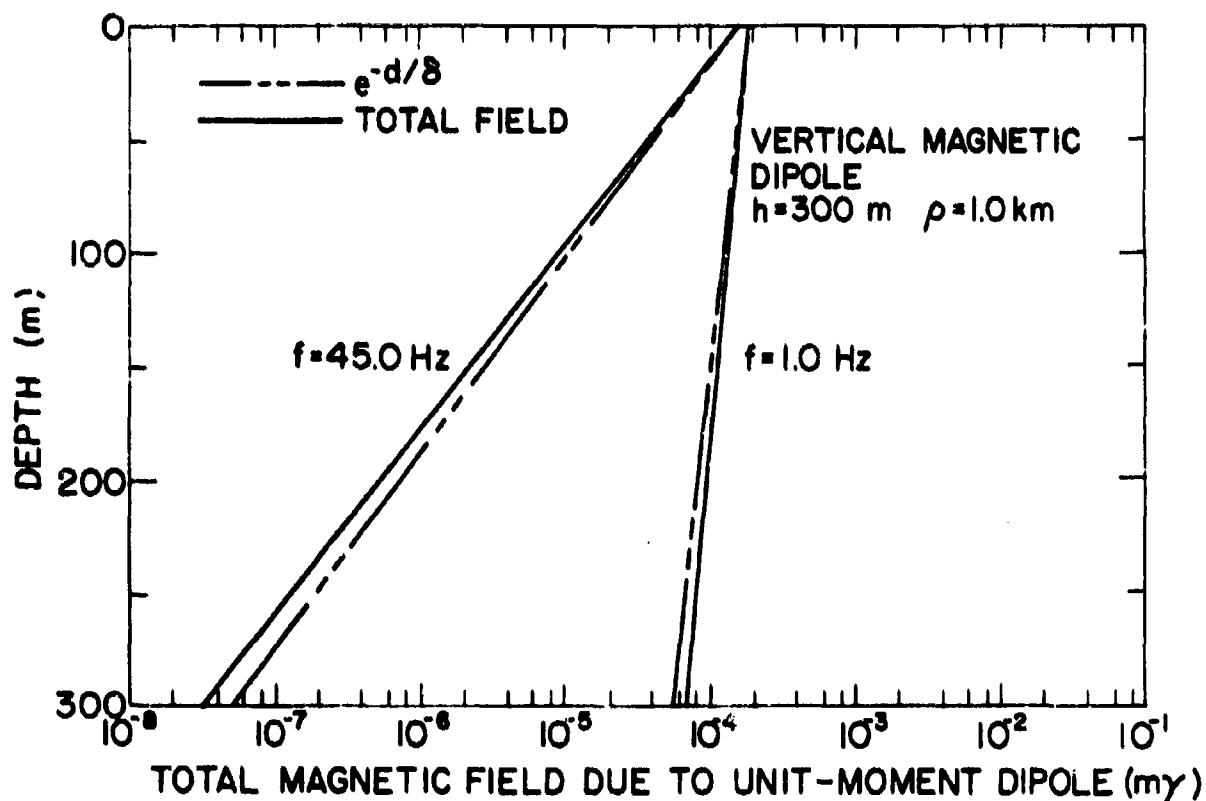
Figure III-1.   Variation of the amplitude of the total magnetic field
produced at depths in the range 0 to 300 m in the sea by an elevated
harmonic VMD of unit moment. The variation is shown at a horizontal
distance of 1.0 km from the axis of the dipole and for the two fre-
quencies 1.0 Hz and 45.0 Hz. The altitude of the dipole above the
sea surface is 300 m, and the sea is assumed to be infinitely deep.
Also shown are the variations that would occur if the field amplitudes
varied as A·exp (d/δ), where A is the amplitude just beneath the
sea surface, d is the depth, and δ is the skin depth.

20

Figure III-2. Variation of the amplitude of the total magnetic field
produced at depths in the range 0 to 300 m in the sea by an elevated
harmonic HMD of unit moment. The variation is shown at a horizontal
distance of 1.0 km from the axis of the dipole and for the two fre-
quencies 1.0 Hz and 45.0 Hz. The altitude of the dipole is 300 m
above the sea surface, and the sea is assumed infinitely deep. Also
shown are the variations that would occur if the field amplitudes
varied as $A \cdot \exp(-d/\delta)$, where A is the amplitude just beneath
the sea surface, d is the depth, and δ is the skin depth.

21

ranges, they nevertheless clearly indicate the validity of what we will call in this work the 'skin depth approximation': the ULF and ELF electromagnetic fields from an elevated magnetic dipole source are attenuated in sea water approximately as $e^{-d/\delta}$, where d is the depth below the surface and δ the skin depth.

2. Total Magnetic Field Produced in the Sea by a VMD

Figure III-3 shows 20 plots of the variation with horizontal distance of the amplitude of total magnetic field produced at different depths in sea water by an elevated harmonic VMD of unit moment (moment $\approx$ 1 A m^2) and a frequency of 1 Hz. The sea is assumed to be infinitely deep, and the heights h, depths d, and horizontal distances ρ (see Figure II-1) cover ranges which we believe include all values of practical interest at the present time. Thus, h takes the values 100, 300, 1000, 3000, and 10,000 m; d takes the values 25, 50, 100, and 200 m; and ρ varies from 1 m to 100 km. Note that the magnetic field of the VMD is symmetrical about the dipole axis and the data in Figure III-3 are therefore applicable at all azimuthal angles.

Both the total magnetic field and horizontal distance scales are logarithmic in order to show in one display data covering many orders of magnitude. Also, the logarithmic display converts a variation of the magnetic field with horizontal distance of the form ρ^{-n}, where n is a constant, into a straight line. Since we expect the magnetic field at large horizontal distances to vary as an inverse power of the horizontal distance, the logarithmic display shows clearly where the transition to the limit of power-law variation takes place.

22
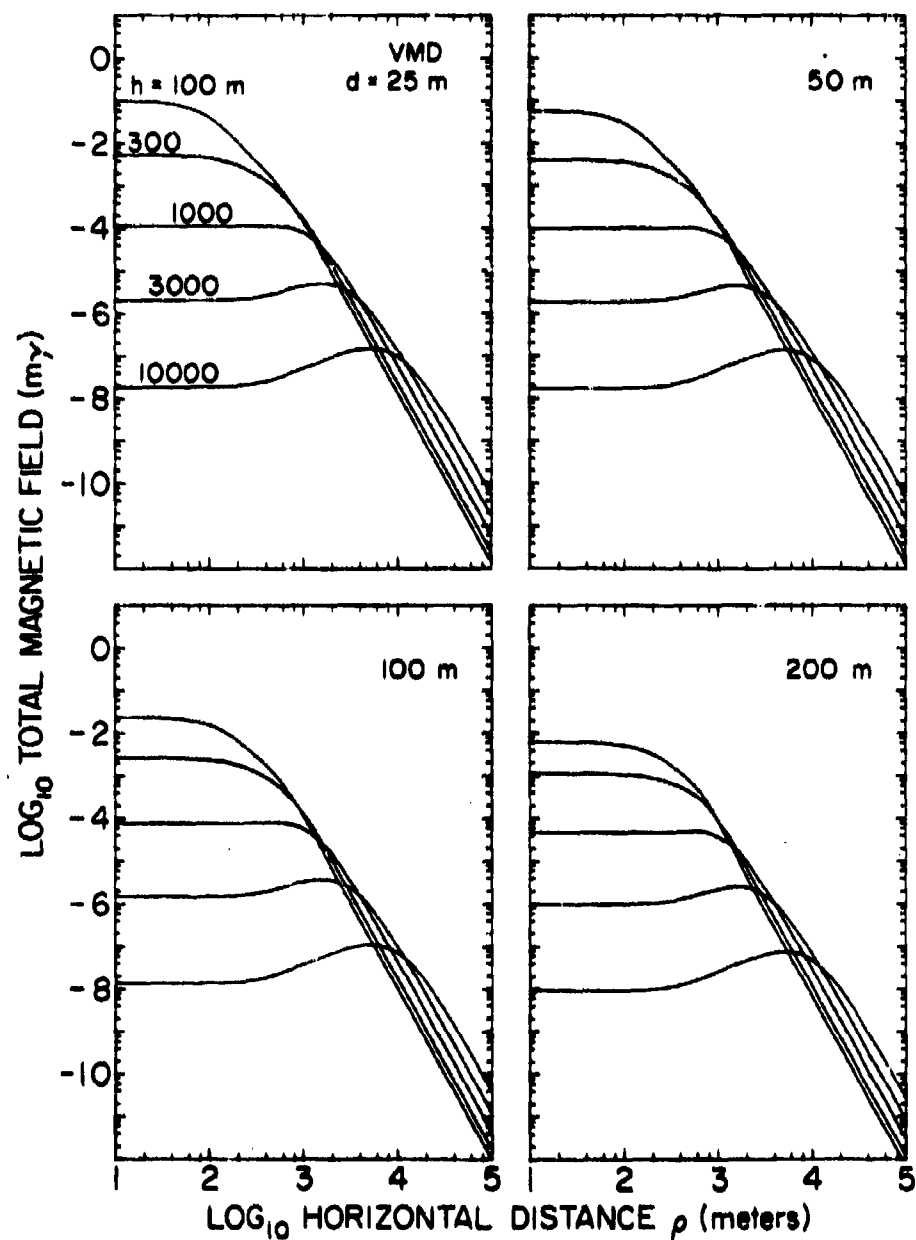
Figure III-3. Variation of the amplitude of the 1 Hz total magnetic field produced at depth d in an infinitely deep sea (σ = 4 mho/m) by a vertical magnetic dipole of unit moment at height h above the sea surface.

In a later section we will compare some of our exact calculated results with those derived by using the approximate expressions of Kraichman (1970). These expressions are accurate for large values of the distance R between the source and receiver. Consequently, in Figure III-3, the range of validity of Kraichman's expressions is not always restricted to the straight line sections at large horizontal distances, as might be expected. We will show that for large h (which automatically implies large R) the curves shown in Figure III-3 are quite closely approximated over the entire range of ρ by the fields derived from the appropriate Kraichman expression.

Each of the curves in Figure III-3 can be considered to be made up of three sections, depending on the form of the curves and the horizontal distance: a 'near' section, an 'intermediate' section, and a 'distant' section. In the near sections the total magnetic field does not change significantly with distance. This lack of variation is most pronounced for a dipole altitude of 1000 m, where, for all depths, the total magnetic field remains approximately constant out to a horizontal distance of approximately 1 km. The intermediate sections represent regions of transition in the distance variation of the total magnetic field. They separate the near sections from the distant sections, where the field varies with distance as ρ^{-n}, i.e., the power law variation discussed above. In Figure III-3 the curves all have the same slope (n = 4) in their distant sections, which agrees with the approximate expressions of Kraichman (1970). For small dipole altitudes ($100 \leq h \leq 1000$ m) the field variation in the intermediate sections declines monotonically as ρ increases and the maximum field

24

amplitude is produced in the sea directly under the dipole. However, for $h > 1000$ m the total magnetic field has a broad maximum in the intermediate sections. Thus, for a VMD at an altitude of 10,000 m, the maximum field is produced at a horizontal distance of about 5 km, and the position of this maximum is very nearly independent of depth over the range shown in Figure III-3.

Comparison of the curves in Figure III-3 shows that at large distances ($\rho > \sim 10$ km) the total magnetic field produced in the sea by the VMD increases as the altitude increases. Thus, even though the field is falling off with horizontal distance as ρ^{-4}, it is possible for the field to increase as the range R increases. For example, at a horizontal distance of 20 km and a depth of 200 m, the total magnetic field produced by a VMD at an altitude of 10,000 m (R = 22.36 km) is greater than the field produced by the same VMD at an altitude of 100 m (R = 20.00 km) by a factor of approximately 25. This large increase in field occurs even though the range increases by 11.8%.

Selected numerical data detailing the amplitudes of the 1 Hz total magnetic field produced at a depth of 200 m by a unit moment VMD at two altitudes (1 km and 10 km) are presented in Table III-1. These data will be used for comparison with the results obtained for the HMD; they will also be used in the last chapter to assess the feasibility of air/undersea communication at frequencies in the ULF range.

Finally, in Figure III-4 we present data illustrating the reduction of the amplitudes of the total magnetic field produced in the sea as the frequency of the elevated VMD is increased above 1 Hz. In this figure we compare the variation with increase of frequency of the total magnetic

25

TABLE III-1

Amplitudes in milligammas of the 1 Hz magnetic field produced at a depth of 200 m in an infinitely deep sea (conductivity 4 mho/m) by elevated unit moment HMD and VMD sources. The data are tabulated for two dipole heights, h = 1 km and 10 km, above the sea surface and for selected values of the horizontal distance ρ in the range 0.1 to 100 km. Powers of 10 are shown in parentheses.

ρ(km)	VMD h (km)		HMD (φ = 0°) h (km)		HMD (φ = 90°) h (km)	
	1	10	1	10	1	10
0.100	4.72 (-5)	9.33 (-9)	5.54 (-5)	8.68 (-8)	5.62 (-5)	8.69 (-8)
0.159	4.73 (-5)	9.52 (-9)	5.35 (-5)	8.68 (-8)	5.53 (-5)	8.68 (-8)
0.251	4.79 (-5)	1.04 (-8)	5.89 (-5)	8.66 (-8)	5.32 (-5)	8.68 (-8)
0.398	4.98 (-5)	1.26 (-8)	3.93 (-5)	8.63 (-8)	4.85 (-5)	8.67 (-8)
0.501	5.07 (-5)	1.47 (-8)	3.23 (-5)	8.59 (-8)	4.46 (-5)	8.65 (-8)
0.631	4.98 (-5)	1.75 (-8)	2.46 (-5)	8.54 (-8)	3.93 (-5)	8.64 (-8)
0.794	4.58 (-5)	2.12 (-8)	1.74 (-5)	8.45 (-8)	3.28 (-5)	8.61 (-8)
1.000	3.82 (-5)	2.60 (-8)	1.20 (-5)	8.31 (-8)	2.56 (-5)	8.56 (-8)
1.259	2.80 (-5)	3.17 (-8)	1.18 (-5)	8.10 (-8)	1.84 (-5)	8.49 (-8)
1.585	1.79 (-5)	3.88 (-8)	1.18 (-5)	7.78 (-8)	1.22 (-5)	8.38 (-8)
1.995	9.98 (-6)	4.70 (-8)	9.49 (-6)	7.29 (-8)	7.52 (-6)	8.21 (-8)
2.512	5.01 (-6)	5.59 (-8)	6.50 (-6)	6.57 (-8)	4.34 (-6)	7.94 (-8)
3.162	2.33 (-6)	6.46 (-8)	3.99 (-6)	5.56 (-8)	2.30 (-6)	7.56 (-8)
3.981	1.02 (-6)	7.16 (-8)	2.28 (-6)	4.21 (-8)	1.28 (-6)	7.01 (-8)
5.012	4.35 (-7)	7.46 (-8)	1.24 (-6)	2.59 (-8)	6.68 (-7)	6.26 (-8)
6.310	1.80 (-7)	7.16 (-8)	6.56 (-7)	9.03 (-9)	3.44 (-7)	5.32 (-8)
7.943	7.37 (-8)	6.17 (-8)	3.40 (-7)	6.23 (-9)	1.75 (-7)	4.24 (-8)
10.00	2.98 (-8)	4.70 (-8)	1.74 (-7)	1.51 (-8)	8.07 (-8)	3.13 (-8)
15.85	4.81 (-9)	1.85 (-8)	4.47 (-8)	1.54 (-8)	2.25 (-8)	1.36 (-8)
25.12	7.68 (-10)	4.73 (-9)	1.13 (-8)	7.19 (-9)	5.68 (-9)	4.55 (-9)
39.81	1.22 (-10)	9.34 (-10)	2.86 (-9)	2.37 (-9)	1.43 (-9)	1.30 (-9)
63.10	1.94 (-11)	1.63 (-10)	7.19 (-10)	6.66 (-10)	3.60 (-10)	3.46 (-10)
100.0	3.07 (-12)	2.68 (-11)	1.81 (-10)	1.75 (-10)	9.03 (-11)	8.90 (-11)

26
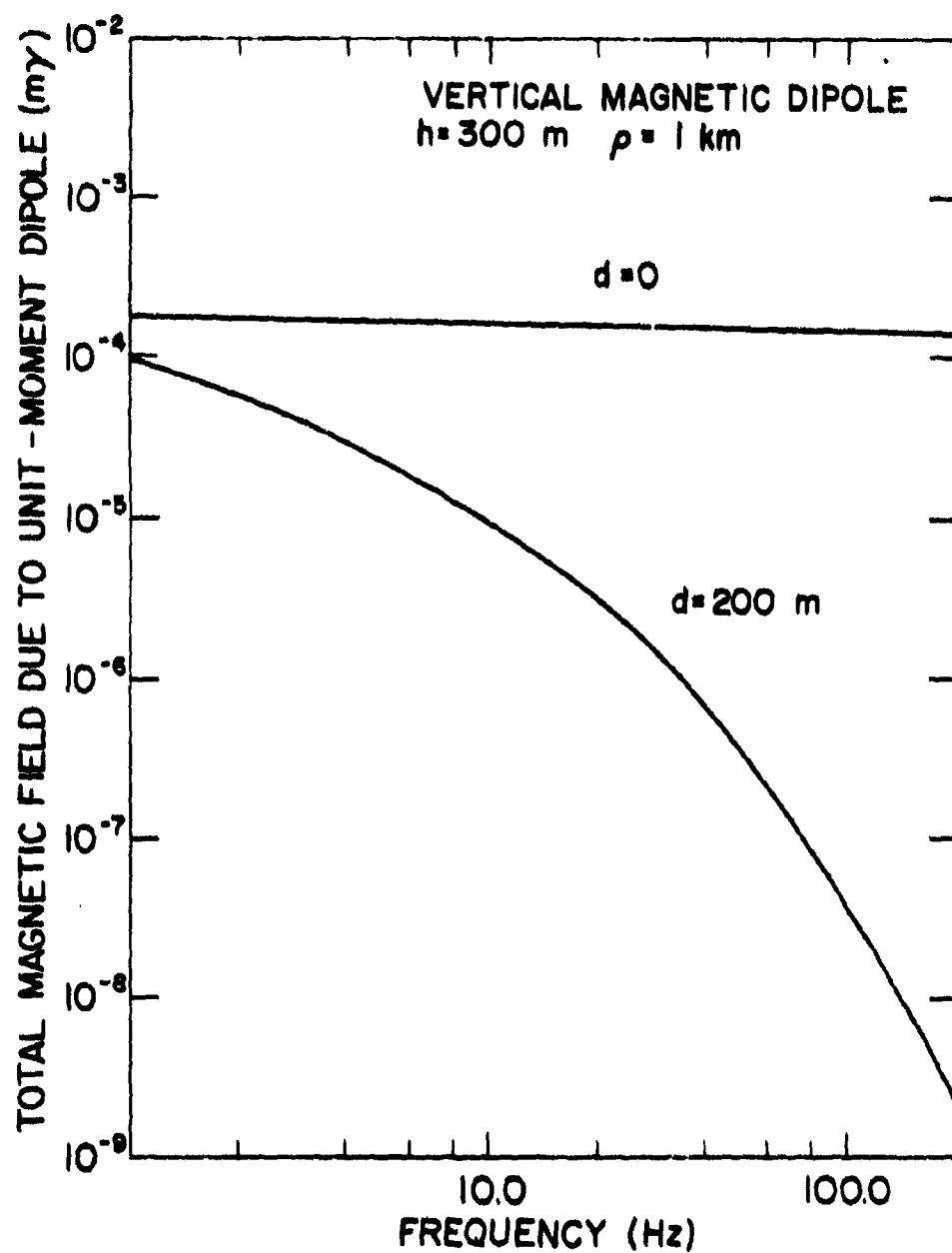
Figure III-4. Data illustrating the effect of an increase of frequency from 1.0 to 200 Hz on the total magnetic field produced on the sea surface (d = 0 m) and in the sea (d = 200 m) by an elevated VMD.

27

field amplitude produced at a horizontal distance of 1 km both on the sea surface (d = 0) and at a depth of 200 m by a unit moment VMD at an altitude of 300 m. The sea is once again assumed to be infinitely deep and the frequency is varied in the range 1 to 200 Hz. For d = 0 there is only a small reduction of the field amplitude as the frequency is increased to 200 Hz. However, for d = 200 the field amplitude, which is about half the field amplitude at the surface for a 1 Hz frequency, drops by nearly five orders of magnitude below the surface field amplitude as the frequency is increased to 200 Hz.

The data in Figure III-4 indicate the importance of the choice of frequency for communication in sea water. If severe signal attenuation is to be avoided, it appears essential to choose a frequency such that the skin depth is roughly of the same magnitude as the maximum depth of the undersea receivers, or is greater than this depth. In Figure III-4 the field amplitude at 200 m declines by only one order of magnitude as the frequency increases from 1 Hz to 10 Hz, i.e., as the skin depth decreases from 251 m to 80 m. Thus, for receivers operating down to a maximum depth of 200 m, a frequency of 10 Hz or less appears most desirable for air/undersea communication if signal attenuation in the sea is to be minimized.

3.   Total Magnetic Field Produced in the Sea by an HMD

Figures III-5 and III-6 show the amplitudes of the total magnetic field produced at different depths in sea water for two azimuthal angles by an airborne HMD of unit moment and a frequency of 1 Hz. As with the VMD, the sea is assumed to infinitely deep, and the heights

28

Figure III-5. Variation of the amplitude of the 1 Hz total magnetic
field produced at depth d in an infinitely deep sea (σ = 4 mho/m)
by a horizontal magnetic dipole of unit moment at height h above
the sea surface. The fields are given in the vertical plane contain-
ing the axis of the dipole.

29

h, depths d, and horizontal distances ρ also have the same values and cover the same ranges as for the VMD. Unlike the VMD, the magnetic field of HMD has a azimuthal angle dependence. The field amplitude is the same for $\phi = 0°$ and $\phi = 180°$, i.e., directly in front of and directly behind the dipole, and it is also the same for $\phi = 0°$ and $\phi = 90°$. At other azimuthal angles the total magnetic field varies smoothly between these two extremes (see equations II-4 through II-6).

The format of Figures III-5 and III-6 is identical with the format for Figure III-3. The curves can also be divided into 'near', 'intermediate', and 'far' sections, although their other properties are significantly different from those of the VMD curves.

Comparing the HMD curves for $\phi = 0°$ and $\phi = 90°$ they are seen to be very nearly identical, particularly in their near sections. However, there are two differences of note: (1) in their intermediate sections the curves for the $\phi = 0°$ case either have distinct minimums (if h is large) or they have corresponding deviations in slope (if h is small), where, in contrast, the curves for $\phi = 90°$ have slopes that vary smoothly with no minimums or deviations, and (2) at large distances ($\rho > 20$ km) the total magnetic field amplitudes of the $\phi = 0°$ case are twice as large as those for the $\phi = 90°$ case. For both values of ϕ, the curves for all different values of h merge into one at large horizontal distances and thus the amplitudes of the 1 Hz total magnetic field become independent of the dipole altitude. Also, the curves become linear at these large distances, with a slope corresponding to a ρ^{-3} power law variation of the field amplitudes. This variation agrees with Kraichman's expressions.
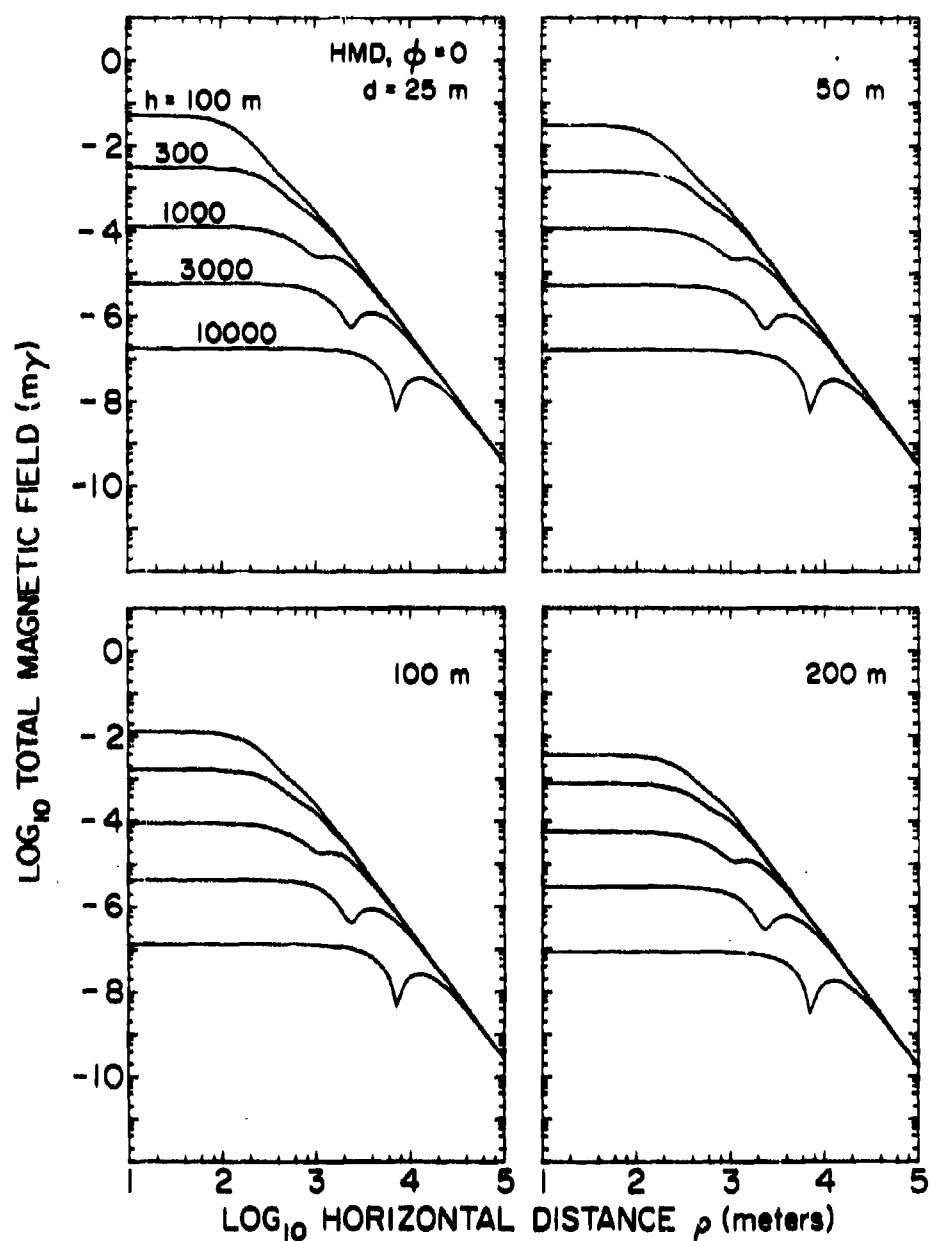
30
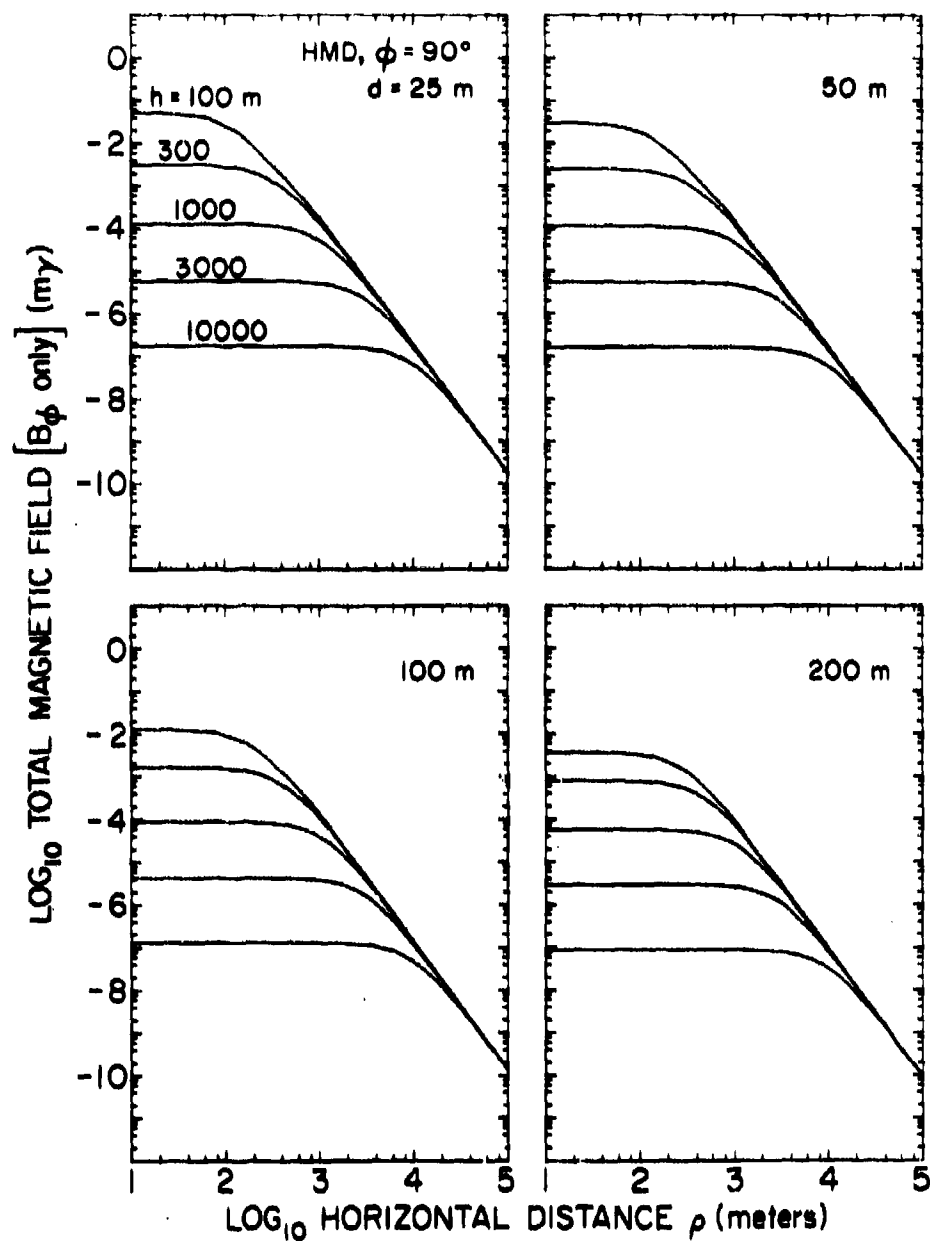
Figure III-6. Variation of the amplitude of the 1 Hz total magnetic field produced at depth d in an infinitely deep sea ($\sigma = 4$ mho/m) by a horizontal magnetic dipole of unit moment at height h above the sea surface. The fields are given in the vertical plane containing the dipole but oriented in a direction perpendicular to the dipole axis.

TABLE III-2.

Ratio [B (HMD, $\phi = 0°$)]/[B (VMD)] of the amplitudes of the 1 Hz total magnetic fields produced at a depth of 200 m in an infinitely deep sea (conductivity 4 mho m^{-1}) by elevated unit moment dipoles. Powers of 10 are shown in parentheses.

ρ (km)	h (km)		ρ km	h (km)	
	1	10		1	10
0.100	1.18 (0)	9.31 (0)	2.512	1.30 (0)	1.18 (0)
0.159	1.13 (0)	9.02 (0)	3.162	1.72 (0)	8.60 (-1)
0.251	1.02 (0)	8.30 (0)	3.981	2.22 (0)	6.88 (-1)
0.316	9.21 (-1)	7.66 (0)	5.012	2.86 (0)	3.47 (-1)
0.398	7.89 (-1)	6.83 (0)	6.310	3.64 (0)	1.26 (-1)
0.501	6.37 (-1)	5.86 (0)	7.943	4.62 (0)	1.01 (-1)
0.631	4.93 (-1)	4.89 (0)	10.00	5.84 (0)	3.21 (-1)
0.794	3.80 (-1)	3.99 (0)	15.85	9.30 (0)	8.30 (-1)
1.000	3.13 (-1)	3.21 (0)	25.12	1.48 (1)	1.52 (0)
1.259	4.22 (-1)	2.55 (0)	39.81	2.34 (1)	2.54 (0)
1.585	6.60 (-1)	2.01 (0)	63.10	3.71 (1)	4.10 (0)
1.995	9.50 (-1)	1.55 (0)	100.0	5.88 (1)	6.55 (0)

32

Selected numerical data detailing the HMD $(\phi = 0^\circ)$ and HMD $(\phi = 90^\circ)$ magnetic field amplitu for $d = 200$ m and $h = 1$ km and 10 km are listed in Table III-1.

4. Comparison of the VMD and HMD Results

The most important difference between the VMD and the HMD from the point of view of air/undersea communication at frequencies in the ULF range is the difference in the rate of fall-off of their field amplitudes at large distances. For the VMD the amplitude of the total magnetic field varies as ρ^{-4} at large horizontal distances, whereas for the HMD the amplitude varies as ρ^{-3}. Thus, the amplitude of the ULF total magnetic field produced in the sea by an elevated VMD falls off more rapidly with distance than does the amplitude of the total field produced by an HMD.

The more rapid decline of the VMD fields with distance is illustrated by the data in Table III-2 for the ratio $[B (\text{HMD}, \phi = 0^\circ)]/[B (\text{VMD})]$. The data in the table are for $f = 1$ Hz, $d = 200$ m, and $h = 1$ km or 10 km. For $\rho = 100$ km and $h = 1$ km the field amplitude produced by the HMD is 59 times as large as the field amplitude produced by the VMD. The ratio declines as h increases; for example, at a dipole height of 10 km the ratio drops from 59 to 6.6.

Although the VMD field amplitudes fall off more rapidly with distance than the HMD fields, there are nevertheless several reasons why the VMD should not be immediately dismissed in favor of the HMD for air/undersea communication. It may be very difficult, for example, to design airborne loop antennas of sufficiently large moment to produce useful ULF signals at the large distances where the HMD fields are

33

superior in strength (for the same dipole moment) to the VMD fields. Under some circumstances it may even be undesirable to have detectable dipole fields at large distances, in which case the VMD could have advantages over the HMD, both because of its more rapid fall off of field strength with ρ and because of certain other features of its fields described below. Finally, installation of a large current loop on an aircraft will involve many practical problems and it is possible that a horizontal loop (VMD) will be easier to install than a vertical loop (HMD).

Two additional features of the VMD fields which could be important in air/undersea communication are (1) their lack of an azimuthal angle dependence and (2) the absence of minimums such as occur in the HMD ($\psi = 0°$) fields (see Figure III-5). The first of these features gives the VMD some advantage over the HMD in that its fields would be more predictable. However, we have already seen that the HMD fields for $\psi = 0°$ and $\phi = 90°$ are nearly identical except for the presence of the minimums in the $\phi = 0°$ case. These minimums are an obvious dis-advantage in the HMD fields and it is interesting to observe that they occur at points occupied by maximums in the equivalent VMD fields. Consequently, the fields of the VMD often exceed those of the HMD in the range of horizontal distances where the HMD minimums occur, and this effect produces the small values of the ratio [B (HMD, $\phi = 0°$)]/ [B (VMD)] tabulated in Table III-2. Another situation where the VMD fields exceed those of the HMD under identical conditions occurs at low h (h < 1000 m) and small horizontal distance, where the VMD fields may be nearly twice those of the HMD.

34

Note that the minimums occurring in the HMD $(\phi = 0°)$ curves are
not related to the unusual "jiggles" observed by Fraser-Smith and
Bubenik (1976) in the ULF/ELF magnetic fields produced at the sea sur-
face by submerged magnetic dipoles. (These jiggles may be caused by
partial cancellation of the fields propagating in the "up-and-over"
mode by the fields propagating directly through the sea water.)
Instead, the minimums occur close to the points where the fields of the
HMD in unbounded free space are entirely vertical, i.e., they are the
field geometry minimums also observed by Fraser-Smith and Bubenik (1976).
Similar minimums would be observed in the curves for the vertical
component of the VMD magnetic field; they do not appear in the total
magnetic field curves for the VMD (Figure III-3) because the horizontal
component is always dominant over the regions in the sea where the
vertical component has its minimums.

5.   Applicability of Kraichman's Approximate Expressions

As we mentioned in Section III-2, Kraichman's (1970) approximate
expressions for the magnetic field produced in the sea by airborne
VMD's and HMD's are accurate provided the source-receiver distance
(i.e., our range, R) is large. How large R should be is illustrated
by Figure III-7, which compares the exact and approximate 1 Hz total
magnetic field amplitudes calculated at a depth of 200 m for a VMD at
two different altitudes, h = 300 m and 1500 m, above the sea. The
exact field values were obtained by using our numerical integration
technique, and the approximate values were obtained by using the
appropriate Kraichman expression.

35

It can be seen that for h = 1500 m there is very little differ-
ence between the curves for the exact and approximate field values,
even for horizontal distances as small as 30 m (i.e., with the receiver
almost directly beneath the VMD). However, for h = 300 m the two
curves begin to differ appreciably once the horizontal distance becomes
less than about 0.6 km. This suggests that the fields derived from the
approximate expressions are accurate provided the source-receiver
distance is greater than about $(500^2 + 600^2)^{1/2}$ m, or 781 m. This
result is in good agreement with the criterion quoted by Fraser-Smith
and Bubenik (1976) for the ULF/ELF magnetic fields produced on the sea
surface by submerged dipoles: the relative error in using Kraichman's
approximate expressions is less than 10% at a frequency of 1 Hz if the
source-receiver distance is greater than 750 m ($\sim 3 \delta$).

6.   Effect of a Sea Floor

The presence of a sea floor with an electrical conductivity less
than that of sea water will alter the magnetic fields produced at points
close to the sea floor by ULF dipole sources above the sea surface.
The following simple argument suggests that the change will be an
increase in the measured total magnetic field. It is expected that the
eddy currents induced in the sea water by the ULF alternating magnetic
field would produce magnetic fields that oppose the inducing field and
thus give a reduced total field. If a sea floor is present just below
the point in the sea where the total field is measured, the eddy
currents beneath the point would be weaker than if sea water alone was
present, assuming the sea floor is less conductive than sea water.
Thus, the measured total field just above the sea floor should be

36
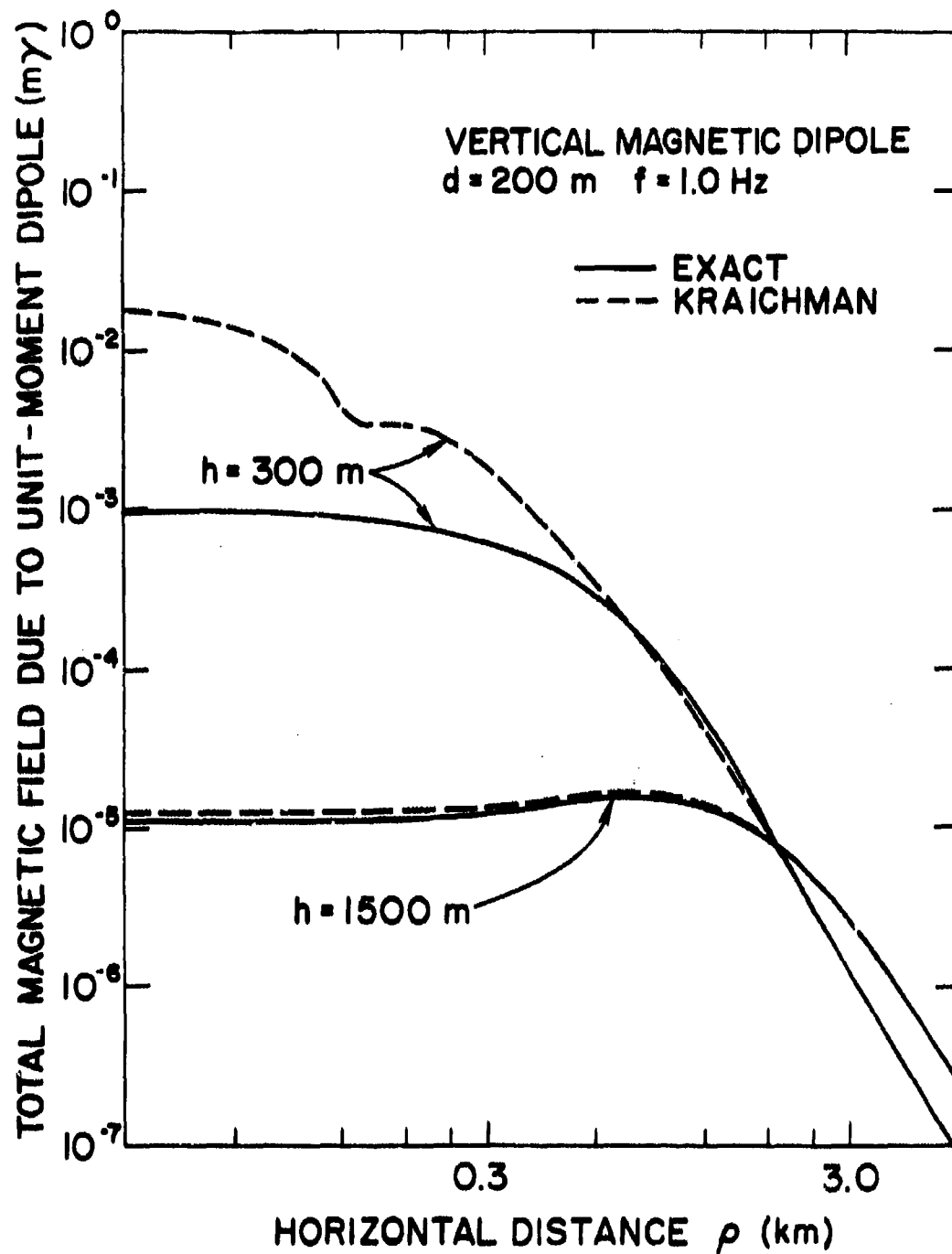
Figure III-7. Comparison of some exact magnetic field data for a VMD with the corresponding approximate values derived from the appropriate Kraichman expression.

larger than it would be at the same point if the sea was infinitely deep. In other words, the ratio B (sea depth = D)/B (sea depth = ∞) should be greater than one, where B (sea depth = D) is the total magnetic field measur·· ct the point above the sea floor and B (sea depth = ∞) is the total magnetic field measured at the same point in an infinitely deep sea.

The simple argument above obviously does not take adequate account of the phases of the various contributions to the total magnetic field at any point and thus at large source-receiver distances it could be expected to be invalid. However, as the data in Figures III-8 and III-9 show, the simple argument gives little guide to the actual variation of the total magnetic field in the presence of a sea floor.

Shown in the two figures are the distance variations of the ratio B (sea depth = D)/B (sea depth = ∞) for a 1 Hz VMD at the two altitudes h = 300 m (Figure III-8) and h = 3000 m (Figure III-9). For each altitude the field ratios are shown for a point on the sea surface (d = 0 m; bottom panel) and for a depth of 200 m (d = 200 m; top panel). The sea depth is varied in the range 10 m to 1000 m and the sea floor is represented by a single semi-infinite layer of conductivity 10^{-2} mho/m. This value of conductivity was chosen for the sea floor because it is significantly smaller than the approximately 4 mho/m conductivity of sea water and yet it is at least one order of magnitude larger than the conductivity of dry rock, which is usually considered less than 10^{-3} mho/m. The value is also consistent with recent conductivity measurements in the range 10^{-1} to 10^{-2} mho/m obtained by the Glomar Challenger at depths of 160 to 400 m in a drill hole in the floor of the Atlantic Ocean (Kirkpatrick, 1977).
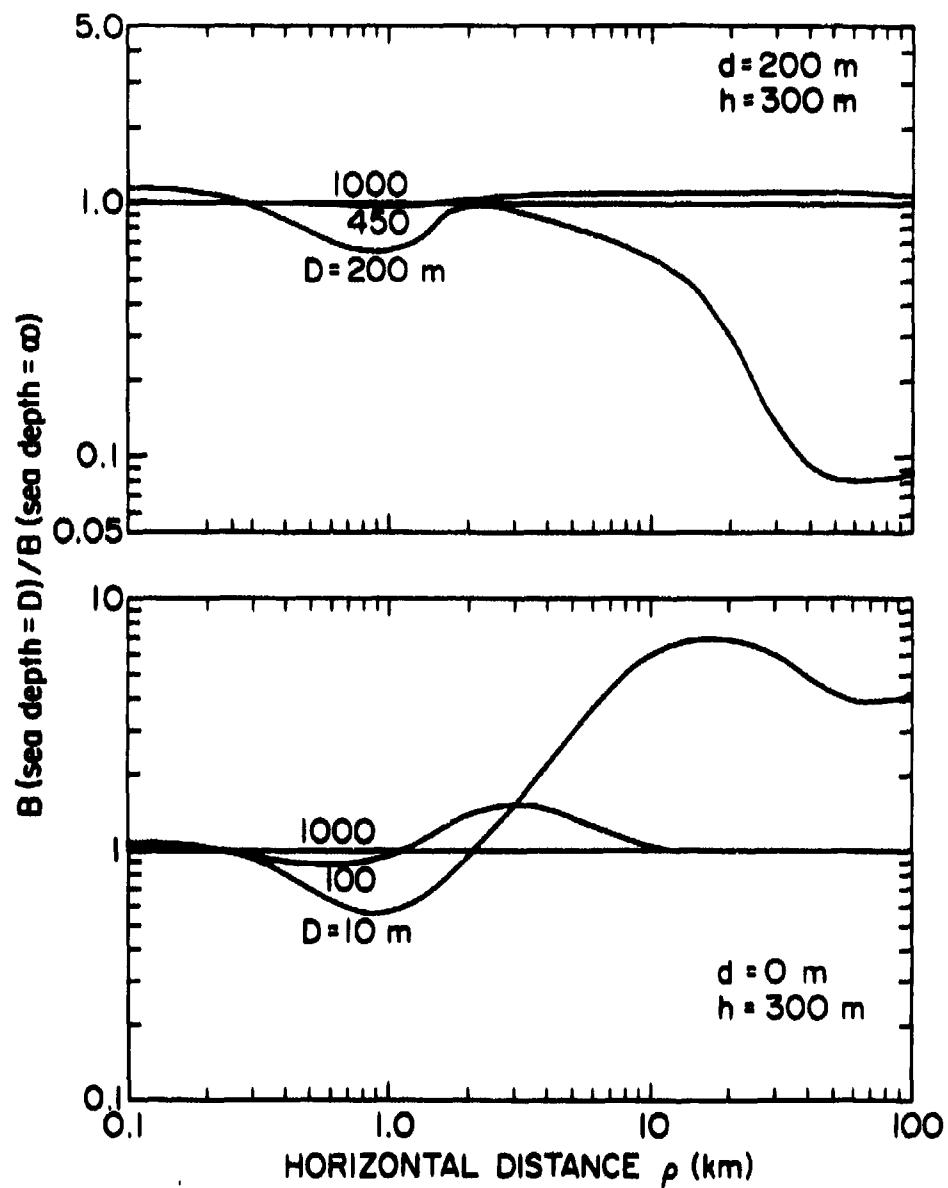
38

Figure III-8.   Changes in the 1 Hz total magnetic field of a VMD caused
by the presence of a sea floor (conductivity 10^{-2} mho/m, depth D).
The VMD is taken to be at an altitude of 300 m and the fields are
computed on the sea surface (d = 0 m) and at a depth of 200 m.
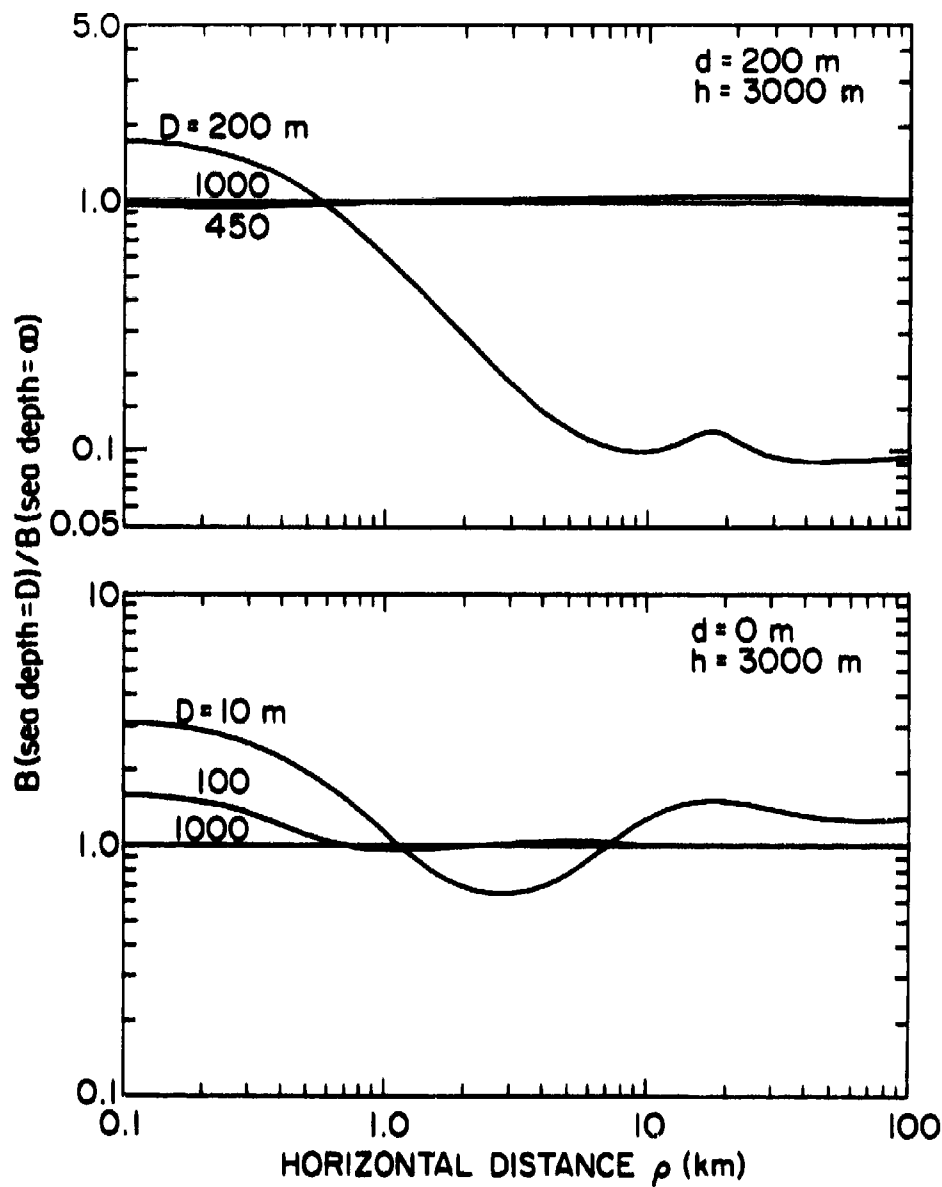
Figure III-9.   Changes in the 1 Hz total magnetic field of a VMD caused
by the presence of a sea floor (conductivity 10^{-2} mho/m, depth D).
The VMD is taken to be at an altitude of 3000 m and the fields are
computed on the sea surface (d = 0 m) and at a depth of 200 m.

40

The data in the two figures suggest that the simple argument is usually valid directly below the VMD. However, for horizontal distances greater than about 400 m, the argument gives little guidance to the actual field behaviour. It is interesting and important to observe that at large horizontal distances the VMD field may be either reduced or increased by up to an order of magnitude by the presence of the sea floor. The largest changes appear to be restricted to field points close to the sea floor. In Figure III-8, for example, the field at a horizontal distance of 50 km is reduced by slightly over an order of magnitude for a point on the sea floor at a depth of 200 m ($d = D =$ 200 m), whereas for the same point but for a sea depth of 450 m ($d = 200$ m, $D = 450$ m) the field is slightly increased by the presence of the sea floor.

These increases and decreases of the total magnetic field of the dipole caused by the presence of a sea floor are of considerable importance for air/undersea communication at frequencies in the ULF range because the largest changes appear to occur at horizontal distances greater than 10 km, where the fields are becoming small and difficult to detect. Thus it would appear that the presence of a sea floor close to the position of the receiver could significantly alter the maximum range of detection of the ULF signal from an airborne magnetic dipole.

In practice, unless the undersea ULF receiver is actually located on the sea floor, the change in the maximum range of detection may not be as marked as indicated by the data in Figures III-8 and III-9. An actual sea floor usually has an upper layer consisting of a variable

41

depth of unconsolidated sediment, which has a conductivity close to that of the sea water itself (Kermabon et al., 1969). For the receiver, this sediment layer could be considered an inaccessible region with electrical characteristics similar to those of sea water, which prevents the undersea ULF receiver from coming close to the effective sea floor (which we suppose has a conductivity that is much smaller than that of sea water). Thus, the large changes in the maximum range of detection for a receiver located on or close to the sea floor are unlikely to be observed, or will not be as large as suggested by the data in Figures III-8 and III-9.

7.   Impedance Changes Produced by the Sea in an Airborne Loop Antenna

In addition to the many factors already discussed in this chapter that affect the 1 Hz total magnetic field produced in the sea by airborne loop antennas (i.e., VMD's and HMD's), the mere presence of the sea itself affects the signal generating capability of an airborne loop antenna by altering its impedance. If the loop impedance is increased greatly by the presence of the sea, it may be difficult, given the limited payload capability of an aircraft, to produce the 1 Hz signal strengths beneath the sea that would be required in a practical air/undersea communication system. In this section we show how the impedance changes can be calculated and we present some representative impedance data for a 12 m radius horizontal loop antenna at various heights above the sea. These data show that the impedance changes produced in the loop antenna by the presence of the sea are unlikely to seriously affect the ULF/ELF signal generating capability of airborne current loops.

42

The loop input impedance Z (not including the ohmic wire resist-
ance) is equal to the voltage per unit driving current induced at the
terminals due to the time-varying magnetic flux linking the loop.
Given a loop of radius a at a height h carrying a current I of
angular frequency ω, the loop input impedance is given by

$$Z = R + iX = V/I = \frac{i\omega}{I} \int_s B_z \, dS$$

where the integral of the vertical magnetic field component B_z is
evaluated over the area S of the loop, R is the resistive component
of the impedance and X is the reactive component. The integral may
be rewritten to give Z in the following form

$$Z = i\omega\mu_0 \pi a^2 \int_0^\infty \left(1 + \frac{\lambda-u}{\lambda+u} \, e^{-2\lambda h}\right) J_1^2 \, (\lambda a) \, d\lambda,$$

which is in agreement with expressions derived by Wait and Spies (1973).
The first term in the above expression represents the self, or primary,
impedance of the loop exclusive of the ohmic wire resistance. This
self impedance is inductive. The second term represents the effect
of the conducting ground (secondary impedance) and contributes both
real (resistive) and imaginary (reactive) parts. As will be shown
presently, this secondary impedance is much smaller than the primary
impedance, and it may thus be regarded as an incremental change in
the total input impedance of the loop.

Since there is no known general closed-form expression for the
second term in the above integral, the integration must be performed
numerically. The secondary impedance was evaluated for a 12 m loop

43

Figure III-10. Incremental increase in the input resistance, as a function of frequency, for a single turn horizontal loop of 12 m radius located at height h (meters) above an infinitely deep sea of conductivity σ = 4 mho/m.

at heights in the range $0 < h < 1000$ m above a conducting "ground" of conductivity $\sigma = 4$ mho/m (i.e., above the sea) for frequencies in the range $10^{-2} \leq f \leq 10^2$ Hz. The real and imaginary parts were separated to give the incremental loop input resistance R and the reactance X due to the induced electric currents in the sea. The reactance was negative; which we interpret as an incremental decrease in the total input inductance of the loop.

In Figures III-10 and III-11 we present our numerical results for the incremental loop input resistance and the incremental loop inductance. Figure III-10 shows the incremental increase in the input resistance, as a function of frequency, for a single turn horizontal loop of 12 m radius located at height h above an infinitely deep sea of conductivity $\sigma = 4$ mho/m. Figure III-11 shows the absolute value of the incremental decrease in the input inductance, as a function of frequency, for the same 12 m radius loop. As would be expected, for a given h, both the incremental resistance and the absolute value of the inductance increase rapidly with frequency, and for a given frequency, these quantities decrease as the height of the loop is increased. Even for a loop on the sea surface (h = 0 m), the values of incremental resistance and inductance are small and, as we will now show, they are also likely to be very small compared to the actual ohmic resistance and self inductance of any practical loop that is used for air/undersea communication.

Suppose the 12 m radius loop consists of a single turn of AWG 10 copper wire. The ohmic resistance of this loop is $0.25\ \Omega$ and its self inductance L, calculated from the formula $L = \mu_o a \left[\ln\left(\frac{8a}{b}\right) - \frac{7}{4}\right]$, where b is the wire radius, is 0.143 mH. Although these values are small, the incremental input resistances and inductances caused by the

45
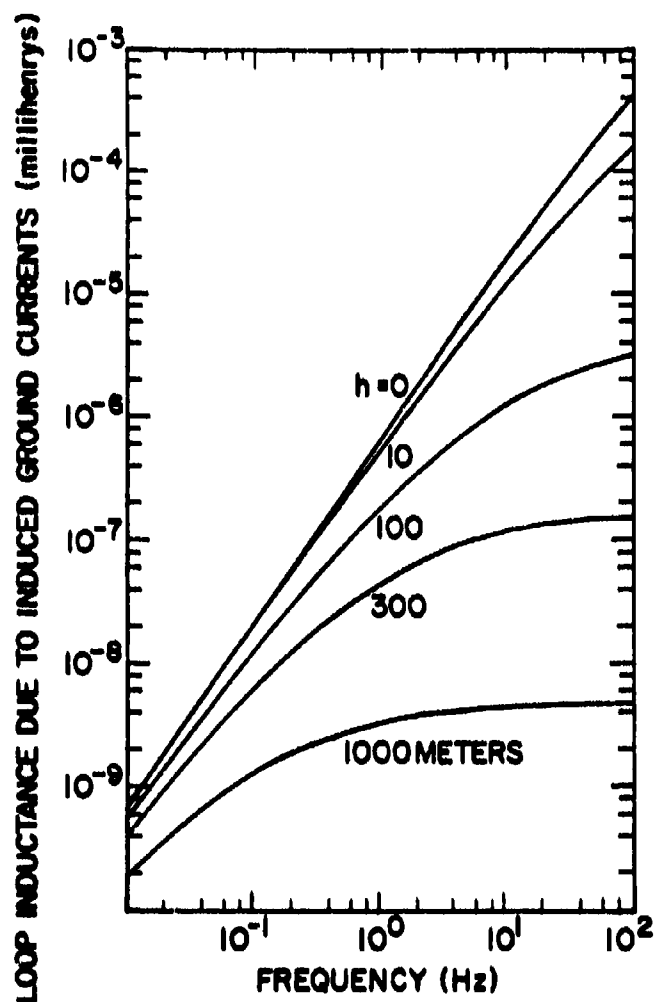
Figure III-11. The absolute value of the incremental decrease in the
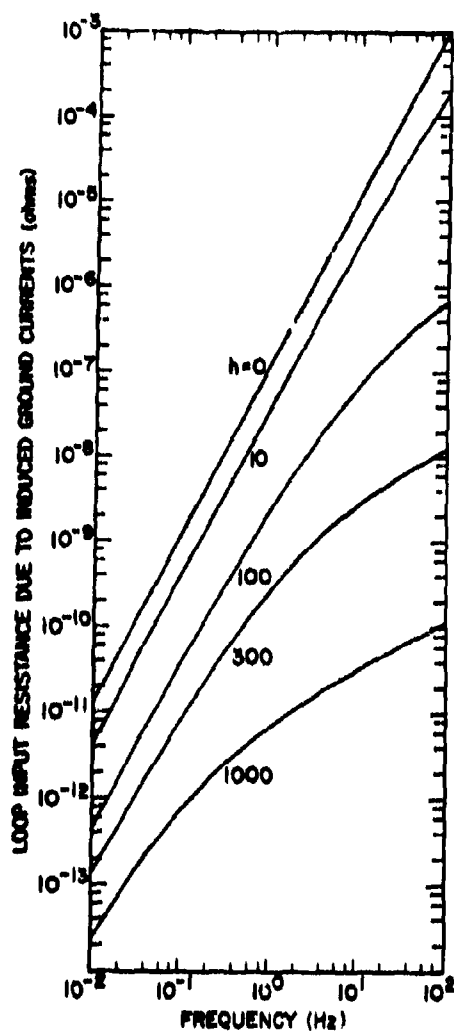 input inductance, as a function of frequency, for a single-turn
  horizontal loop of 12 m radius located at height h above an
  infinitely deep sea of conductivity σ = 4 mho/m.

46

sea water are many orders of magnitude smaller. For example, if the
12 m loop is being driven at a 1 Hz frequency and is at an altitude
of 1000 m above the sea surface, the incremental loop input resistance
is close to 6×10^{-12} Ω, which is clearly negligible compared to the
0.25 Ω ohmic resistance of the loop. For the same loop, the incremental
loop inductance caused by the sea is about -3×10^{-9} mH, which also is
negligible compared to the 0.143 mH self-inductance of the loop.

The numerical data plotted in Figures III-10 and III-11 are for a
single-turn loop and should be scaled in proportion to the square of
the number of turns for a multiturn loop. The self-inductance of an
isolated multiturn loop also scales as the square of the number of
turns and thus, for a multiturn loop above the sea, the incremental
loop inductance will always remain small compared to the self-inductance
even if the number of turns is very great. The ohmic resistance of a
multi-turn loop, on the other hand, scales as the number of turns, and
it would be possible for the incremental input resistance to approach
and even exceed the ohmic resistance for a multiturn loop with a great
many turns above the sea. In the present case, however, the number of
turns required for the resistances to become comparable ($\sim 10^6$) is
so great that the loop would impractical. Thus, we conclude that
impedance changes produced by the sea in an airborne loop antenna are
unlikely to be significant for air/undersea communication.

IV. POSSIBLE MAGNETIC MOMENTS OF AIRBORNE ULF CURRENT LOOPS

1. Introduction

The amplitude of the undersea electromagnetic field generated by an
airborne dipole antenna is proportional to the moment of the dipole.
For a magnetic dipole formed by a conducting loop enclosing an area A,
the moment is given by $m = IA$, where I is the total current through
a cross section of the loop. Thus the moment, and therefore the maximum
range of communication, of a practical loop antenna is limited by the
physical size of the antenna and by the total available power. These
constraints are particularly rigorous on an aircraft, where the size,
weight, and available power are subject to definite restrictions. It
is the purpose of this chapter to estimate the maximum practical dipole
moment attainable using, as a representative standard aircraft, the
Lockheed P-3 Orion. We shall consider both conventional and superconduct-
ing loops.

2. Constraints Imposed by the Aircraft

According to Jane's All the World's Aircraft, the Lockheed P-3 Orion
is the current American standard aircraft for locating and tracking sub-
marines. Essentially a modified Electra airliner. It can carry a 9100 kg
expendable load, is very maneuverable, and can operate at altitudes rang-
ing from 100 m to 8600 m. Its wingspan is 30.4 m and its overall length
is 35.6 m. The electrical power supply includes three 60 kVA 400 Hz AC
generators and an additional 60 kVA auxiliary power unit.

3.   Loop Antenna Design Considerations

We begin with the expression for the loop magnetic moment,

$$m = AI$$
$$= ANi$$

where i is the current in each of N conductors passing through a cross section of the loop. The loop area A is limited by the size of the aircraft and may be regarded as constant. We therefore design around the Ni product, which should be as large as possible within the constraints of allowable conductor weight and generator capacity.

The power fed to the loop terminals is a complex quantity, representing the real power dissipated in the loop conductors and the reactive power due to the loop inductance. Since the loop inductance is very difficult to determine (its computation is complicated by the presence of the metal aircraft, and it seems best determined experimentally from a model), we estimate a reasonable power factor to be 0.5. Thus, given a conductor of DC resistance ρ per unit length, the total (real plus reactive) power drawn from the generator is $2i^2 \rho \alpha N\sqrt{A}$ volt-amperes, where $\alpha = 2\sqrt{\pi}$ for a circular loop and $\alpha = 4$ for a square loop.

The Ni product can be apportioned in several ways: (1) A single conductor wound N times around the loop. This configuration gives a relatively high inductance, requires a high driver voltage but low terminal current, and is subject to complete failure if the conductor breaks. (2) N single conductors wound about the loop and connected in parallel at the terminals. This results in a lower inductance, low driving voltage but high terminal current, and is relatively unaffected by breaks in a limited number of conductors. (3) N_1 single-conductor

50

loops of (N/N_1) turns connected in parallel. This compromise gives an intermediate inductance and allows the terminal voltage and current to be adjusted to the generator's characteristics by varying N_1. All of the above combinations dissipate the same real power, and have the same weight for a given loop moment and conductor size. For reference, the weight of the conductors in a loop antenna is $W' \alpha N \sqrt{A}$, where W' is the weight per unit length of the conductor.

The conductor current i is constrained by power supply considerations, and also by the conductor size. Electrical codes and practice fix an upper limit on the order of $0.1 I_f$, where I_f is the wire fusing current given by $I_f = Kd^{3/2}$, where K is a constant corresponding to the wire material, d is the wire diameter given by $d = 0.0825 \exp (- 0.116 \text{ AWG})$ m, and AWG is the American Wire Gauge size of the conductor (ITT, 1968, p. 4-55).

Considering the large number of variables involved, there appears to be no single design formula leading to an optimum loop of greatest moment given the area, weight, and power limitations. A computer optimization approach would probably be profitable in the design of an actual antenna, but this was not attempted in this study. Instead, a digital computer was used to determine the characteristics of many possible designs, subject to the appropriate constraints.

For the P-3 Orion we take: (1) Total conductor weight = expendable load = 9100 kg; (2) Power available = 120 kVA (2 generators in service, 1 in reserve); real power available = 120/2 = 60 kW; (3a) Loop area = 452 m², corresponding to a loop strung from nose to wingtip to tail to wingtip to nose (VMD); and (3b) Loop area = 9.3 m², corresponding to a loop wound around the fuselage (HMD).

51

The estimated attainable loop moments under these conditions are listed in Table IV-1. It is apparent that the maximum attainable moment of a non-superconducting loop probably lies in the range 10^7 - 10^8 A m^2.

Table IV-1. The estimated maximum feasible moments of ULF transmitting loops on a P-3 Orion aircraft, using non-superconducting loops and a continuous square wave drive current. Conductor current $i = 0.03$ I_f; smaller currents give lesser moments, while larger currents require excessive power.

	M (A m^2)	N	i(A)	AWG	Weight (kg)	Power (kW)
	COPPER WIRE					
VMD	1.0×10^7	2262	10.0	10	8.997	62
HMD	1.7×10^6	17752	10.0	10	9,000	63
	ALUMINUM WIRE					
	M (A m^2)	N	i(A)	AWG	Weight (kg)	Power (kW)
VMD	1.4×10^7	738	42.1	0	8,996	58
HMD	2.3×10^6	5792	42.1	0	9,000	58

Using superconducting technology, the real power required to drive the loop is almost negligible; and the limitation is the reactive power which the generator can supply to the essentially inductive load. However, in this case the horizontal loop size probably must be reduced to allow for the necessary cryogenic cooling apparatus, thus reducing the loop area A and the vertical dipole moment for a given Ni product. Nevertheless, the attainable moment may be quite large; an existing superconducting loop of 1.5 m diameter (Morrison and Dolan, 1973) gives a moment of 10^5 A m^2 at 45 Hz using a conservative current drive, and weighs less than 1 ton. Extrapolating this data to higher currents and larger sizes, it seems possible that a superconducting transmitter loop could attain moments of 10^8 - 10^9 A m^2.

4. Conclusions

Vertical magnetic dipole moments on the order of 10^7 - 10^8 A m^2 appear to be attainable using non-superconducting loops on a P-3 aircraft with a continuous square wave drive current. The practical horizontal dipole moment is nearly an order of magnitude less. These moments could probably be more than doubled if the antenna were driven by a pulsed current waveform at a duty cycle of 50% or less. A superconducting loop is expected to attain a moment of 10^8 - 10^9 A m^2, owing to its reduced power requirements. The gain offered by superconducting technology would be especially pronounced in the case of the horizontal dipole (loop in vertical plane), whose area would not need to be substantially reduced in order to accommodate the cryogenic cooling apparatus.

4. Conclusions

Vertical magnetic dipole moments on the order of 10^7 - 10^8 A m^2 appear to be attainable using non-superconducting loops on a P-3 aircraft with a continuous square wave drive current. The practical horizontal dipole moment is nearly an order of magnitude less. These moments could probably be more than doubled if the antenna were driven by a pulsed current waveform at a duty cycle of 50% or less. A superconducting loop is expected to attain a moment of 10^8 - 10^9 A m^2, owing to its reduced power requirements. The gain offered by superconducting technology would be especially pronounced in the case of the horizontal dipole (loop in vertical plane), whose area would not need to be substantially reduced in order to accommodate the cryogenic cooling apparatus.

V. FEASIBILITY OF AIR/UNDERSEA COMMUNICATION WITH AIRBORNE LOOP ANTENNAS

By combin'ng the results obtained in Chapter III (results of cal-
culations of the undersea fields) and Chapter IV (magnetic moments of
possible airborne current loops) we are now able to estimate the horizon-
tal ranges over which air/undersea communication at 1 Hz with airborne
loop antennas may be feasible.

1. Minimum Detectable 1 Hz Magnetic Field Amplitude

Conventional ULF recording systems typically use induction loop
antennas as sensors. These induction loops may consist of long solenoids
with a core of ferromagnetic material (e.g. mumetal) or large-diameter
air-cored coils. An induction loop antenna measures a single component
of the magnetic field and measurement of the total magnetic field
requires three of these antennas in a mutually orthogonal configuration.

The internal noise level in the induction loop systems varies from
system to system. A representative noise level is 0.3 $m\gamma/\sqrt{Hz}$ in the
0.1 to 10 Hz band (Buxton and Fraser-Smith, 1974). This noise can be
reduced substantially by using superconducting magnetometers as ULF
receivers (Buxton and Fraser-Smith, 1974; Fraser-Smith and Buxton,
1975). However, while there may be some advantage to reducing the in-
ternal noise below 0.3 $m\gamma/\sqrt{Hz}$, substantial further reduction is probably
not justified in the presence of the natural ULF noise background. The
level of the natural ULF noise background is greatly variable: it varies
in particular with time of day, frequency, location on the earth's
surface, and with the state of geomagnetic disturbance. The middle
latitude study by Fraser-Smith and Buxton (1975) shows the nighttime

55

background level in the 0.1 to 10 Hz band varying from about 20 $m\gamma/\sqrt{Hz}$ at 0.1 Hz to about 0.4 $m\gamma/\sqrt{Hz}$ at 10 Hz during geomagnetically quiet periods (the background varies approximately as f^{-1} throughout the frequency range 10^{-4} to 100 Hz). During the day, and during intervals of geomagnetic disturbance, the background noise level increases. At most times there is a minimum of activity in the 3 to 7 Hz band, and the noise level in this band is typically less than 1.0 $m\gamma/\sqrt{Hz}$. At 1 Hz the noise level is usually less than 2.0 $m\gamma/\sqrt{Hz}$ (the noise level can be up to 100 times larger during the course of relatively infrequent Pc 1 geomagnetic pulsation events (Jacobs, 1970)). Because the noise level increases rapidly as the frequency drops below 0.1 Hz, it appears that the best frequency band for ULF air/undersea communication is 1 to 6 Hz.

For ULF measurements in the sea, and particularly near the sea surface, the motion of sea waves in the geomagnetic field provides an additional source of ULF noise (e.g., Warburton and Caminiti, 1964, Podney, 1975). The amplitude of both this noise and of the natural ULF background declines with depth in the sea, although the rate of decline of the wave-induced noise may not be the same as the $e^{-d/\delta}$ attenuation that is to be expected for the natural background (c.f. Section III-1). Measurements of the wave-induced ULF noise do not appear to have been made in the 1 to 6 Hz frequency band. However, measurements at lower frequencies suggest that the noise occurs predominantly at frequencies below 0.1 Hz, and that at depths of 100 m or greater the wave-induced noise in the 1 to 6 Hz band has an amplitude that is much less than 1 $m\gamma$ (Maclure et al., 1964).

56

Thus, for submerged ULF receivers at rest, we conclude that a 1 m_γ total magnetic field amplitude from an airborne loop antenna operating at a 1 Hz frequency can probably be detected with little difficulty in the presence of both internal ULF receiver noise and natural ULF background noise, provided the receivers are sufficiently deep in the sea to avoid wave-induced noise at the operating frequency. Large amplitude Pc 1 geomagnetic pulsation events may, on comparatively rare occasions, produce a total magnetic field amplitude much greater than 1 m_γ at 1 Hz. However, the characteristics of the signal from the airborne loop antenna will be so different from those of the Pc 1 pulsation event (e.g. Fraser-Smith, 1977) that there should be little difficulty distinguishing the two ULF signals.

If the submerged receiver is in motion, the receiver sensitivity may be decreased substantially by a variety of motion-induced noises. ULF receivers using solenoids or coils as sensors (including superconducting magnetometers) are particularly susceptible to motion induced noise. Because they respond with high sensitivity to components of the magnetic field, small angular displacements of the sensors caused by vibration or other motion can introduce large noise components. One possible solution to this problem is to use total field magnetometers as ULF receivers. However, present total field magnetometers do not achieve the high sensitivity of the component magnetometers: they are, in particular, at least several orders of magnitude less sensitive than present superconducting magnetometers.

There have been two important recent developments in response to the motion noise problem: (1) the Naval Research Laboratory (NRL) is

57

investigating the possibility of combining operation of a three-axis superconducting magnetometer on a towed stabilized platform with a signal processing method that sums the squares of the three component measurements to obtain a total field output (Wolfe et al., 1974; Davis et al., 1977), and (2) magnetic field loop antennas in the form of long towed cables, with superior noise characteristics for this type of antenna, have been designed and tested (Burrows, 1975). These developments were stimulated by the proposal to use ELF signals for submarine communications, i.e., by the proposed Sanguine and Seafarer ELF communication systems, and the frequencies of interest lie in the approximate range 30 to 130 Hz. These frequencies are substantially higher than the ULF frequencies ($\sim$ 1 Hz) being considered for air/undersea communication in this report, and thus it is not always possible to relate the progress being made in motion-noise reduction to the ULF range. Nevertheless, NRL has demonstrated considerable progress toward achieving their required receiver sensitivity of 10^{-2} mγ/$\sqrt{Hz}$ in the 30 to 130 band. This sensitivity is over an order of magnitude greater than the sensitivity of the best conventional ULF receivers at rest. Considering the flat frequency response of superconducting magnetometers, it is reasonable to assume that the same high sensitivity could be achieved in the 0.1 Hz to 10 Hz band.

We therefore conclude that a conventional ULF receiving system at rest in the sea can probably easily detect a 1 mγ total magnetic field amplitude at a frequency of 1 Hz provided wave-induced noise can be ignored. For a ULF receiving system in motion, motion-induced noise can become an important problem if the ULF receiving system uses induction

loop antennas as sensors. However, recent progress at NRL suggests
that a towed three-axis superconducting magnetometer can be designed to
measure a 1 mγ total magnetic field amplitude at 1 Hz. Thus, in the re-
mainder of this chapter we will adopt a 1 mγ total magnetic field ampli-
tude that can be detected by a submerged ULF receiver.

2. Maximum Distances for Air/Undersea Communication at 1 Hz

Based on the discussion in Chapter 4, we adopt 10^7 to 10^9 A m^2
as a possible range of maximum moments for airborne VMD's and HMD's.
Given a minimum detectable total magnetic field amplitude on the order
of 1 mγ (at a 1 Hz frequency), as discussed in the previous section, we
can now calculate the ranges of horizontal distances over which air/
undersea communication at 1 Hz using airborne current loops will be
possible.

For most airborne loop/undersea receiver configurations, the range
of horizontal distances can be specified completely by a single value of
the distance, ρ max, which is the maximum horizontal distance at which
the airborne loop produces a 1 mγ total magnetic field amplitude (for a
1 Hz frequency) at the submerged ULF receiver. With the exception of a
few high-altitude VMD configurations, the total magnetic field amplitude
at any horizontal distance less than ρ max will be greater than 1 mγ.

In the exceptional VMD cases, the total magnetic field amplitude
falls below 1 mγ for some ρ min < ρ max. As shown by the data in Figure
III-3, a high-altitude VMD (3 km $\leq$ h $<$ 10 km) may produce a detectable
total magnetic field amplitude over the more limited range ρ min $\leq$ ρ $\leq$ ρ
max, where ρ min > 0. For example, suppose a 0.5 × 10^8 A m^2 VMD is
located at an altitude of 10,000 m and its 1 Hz total magnetic field

59

is being measured by a ULF receiver at a depth of 200 m. Scaling distances approximately from the appropriate curve in Figure III-3, total magnetic field amplitudes greater than 1 mγ are produced only in the annular area beneath the VMD defined by 800 m < ρ < 15 km. In this case ρ min $\approx$ 800 m and there is a "dead" area directly beneath the VMD where the total magnetic field amplitude is slightly less than the detectable level of 1 mγ.

It is clear from Figure III-3 that such "dead" areas beneath the transmitter occur only under limited conditions. Therefore, unless specifically stated otherwise, in the follow discussion it is to be assumed that a receivable field intensity exists at all values of ρ < ρ max.

Referring again to Figure III-3 for the VMD, we assume our ULF receiver is located at a depth of 200 m (maximum attenuation), and we find the maximum horizontal distances for total magnetic fields of 10^{-7} mγ and 10^{-9} mγ, which correspond to a 1 mγ field for VMD moments of 10^7 A m^2 and 10^9 A m^2, respectively. The range of ρ max thus obtained for the VMD at an altitude of 3000 m is 9.0 km to 30.2 km. (These values, and the following values for ρ max, are derived from the numerical data used to prepare Figures III-3 and III-5; they are not scaled directly from the figures). For a VMD at an altitude of 10,000 m the total magnetic field produced by a 10^7 A m^2 moment is everywhere less than 1 mγ and is therefore judged to be unreceivable. However, if the moment of the dipole is 10^9 A m^2, the total magnetic field exceeds 1 mγ out to a horizontal distance of 39.0 km.

These results show the importance of having as large a magnetic moment as possible for the VMD if large values of ρ max are desired. Also, the results show that, for a given VMD moment, ρ max can be increased (with a limit set by the dipole moment) by increasing the altitude of the VMD.

If we now assume our ULF receiver is located at a depth of 100 m, the horizontal distances over which air/undersea communication at 1 Hz is possible are increased over the corresponding distances for a ULF receiver at a depth of 200 m. However, because of the comparatively low attenuation of 1 Hz electromagnetic fields in sea water, the increase in distance achieved by halving the receiver depth is not as substantial as may be expected. For VMD's moments in the range 10^7 A m^2 to 10^9 A m^2 located at an altitude of 1000 m, the range of maximum distances for air/undersea communication is 8.0 km to 26.0 km. The corresponding range of ρ max for the VMD at an altitude of 3000 m is 10.0 km to 33.1 km. When the VMD is at an altitude of 10,000 m, a 10^7 A m^2 moment is insufficient to produce detectable total magnetic field amplitudes (ρ max = 0). However, when the VMD moment is 10^9 A m^2, detectable total magnetic field amplitudes are produced at all horizontal distances out to ρ max = 43.2 km. Comparing the maximum distances for communication using a 10^9 A m^2 VMD, we see that the ρ max of 39.0 km for a ULF receiver at a depth of 200 m is increased to 43.2 km if the ULF receiver is at 100 m: an increase of only 11 percent.

As noted in Section III-4, the total magnetic field produced in the sea by an elevated VMD falls off more rapidly at large distances than does the field produced by an HMD. We would therefore expect the

61

maximum horizontal distances obtained for air/undersea communication
with an HMD to be larger than those obtained for a VMD of the same
moment. In fact, under the same conditions as for the VMD above, the
values of ρ max are approximately doubled for an HMD source if the total
magnetic fields are measured in the $\phi = 0°$ plane. For example, suppose
the ULF receiver is at a depth of 100 m and is located directly ahead
of a 10^9 A m^2 HMD (i.e., $\phi = 0°$). The maximum horizontal distance for
an air/undersea communication at 1 Hz in this example is 64.0 km, and
this value of ρ max applies for the HMD at any altitude in the approx-
mate interval 1 km to 10 km. For comparison, we obtained ρ max = 26.0
km for a 10^9 A m^2 VMD at an altitude of 1 km and ρ max = 43.2 km for the
same VMD at an altitude of 10 km (in both cases the ULF receiver was at
a depth of 100 m). For the same HMD ($\phi = 0°$) source, but with the ULF
receiver at a 200 m depth, ρ max = 56.2 km for all HMD altitudes in the
approximate interval 1 km to 10 km.

These data emphasize a further distinction between the VMD and HMD
fields that is not discussed in Section III-4, i.e., at large distances
the HMD total magnetic field does not increase with increase of the
dipole altitude, whereas, as we have just observed, increasing the
altitude of the VMD can increase the total magnetic field it produces at
large distances. In Figures III-5 and III-6 the lack of an altitude
dependence of the HMD fields at large distances appears as a merging of
the curves at large ρ.

62

3. Limited Ranges for Air/Undersea Communication at 1 Hz

In most communication systems the primary object is to obtain the largest possible range of communication for a given input power. However, under some circumstances it could be desirable to limit the range of communication. We have already noted, in the previous section, how air/undersea communication at 1 Hz with a VMD could be restricted to an annular area beneath the VMD. However, the conditions for producing this limited range of communication involved very specific altitudes and moments for the dipole source.

It is also possible, as the data in Figure III-3, III-5, and III-6 show, to limit communication to a small circular area directly beneath the VMD or HMD source. Because the conditions for producing this limited circular area of communication are much less strict than those for producing the limited annular area of communication, it is conceivable that the ability to restrict air/undersea communication to a small area could have practical use.

The first requirement for obtaining the small area of communication is for the aircraft to fly at a low altitude. For example, suppose the ULF source is a VMD and that its altitude is 300 m. At this low altitude the flat portions of the curves in Figure III-3 extend out only to horizontal distances on the order of 200 to 400 m. Now, if the dipole moment is reduced (this is the second requirement) from its assumed value in the range 10^7 A m^2 - 10^9 A m^2 to a value near 10^3 A m^2, the data in Figure III-3 show that air/undersea communication can be limited to the flat portions of the h = 300 m curves, i.e., communication is restricted to a circular area of radius approximately 400 m directly

63

beneath the VMD. This result is essentially independent of the depth of the ULF receiver in the range 0 m to 200 m, although the 1 Hz signal will be close to 1 m$_\gamma$ and only just observable at a depth of 200 m for a 10^3 A m^2 VMD. Examination of Figures III-5 and III-6 shows that the same limited area of communication can be obtained with an HMD source.

Limitation of air/undersea communication to a circular area of only 400 m radius beneath an airborne dipole source may not be desirable in practice in view of the additional requirements imposed on the air/ undersea communication link by the speed of the aircraft and the low data rate for communication at 1 Hz. The above example is only illus- trative. The important conclusion remains, however, that air/undersea communication at 1 Hz using airborne loop antennas can be restricted to submerged ULF receivers in a circular area of known size directly be- neath the aircraft, and that the size of this circular area can be con- trolled within wide limits by variation of (a) the dipole moment and (b) the altitude of the aircraft.

4.   Conclusions

In this report we have presented arguments and data to justify two basic conclusions:

(i)   Horizontal or vertical airborne loop antennas
        with magnetic moments in the range 10^7 A m^2
        to 10^9 A m^2 appear to be attainable with
        present aircraft power and payload capability.
        It is assumed that the current in these air-
        borne loop airborne loop antennas can be
        switched or alternated at a 1 Hz frequency.

64

(ii)   An alternating total magnetic field with a
frequency of 1 Hz and an amplitude of 1 mγ
can be detected beneath the sea by using
present induction loop or superconducting ULF
receivers at rest or, with some further develop-
ment, by using a towed stabilized three-axis
superconducting magnetometer system.

Following these two basic conclusions, we further conclude:

(iii)   Air/undersea communication at 1 Hz is possible
using horizontal or vertical airborne loop
antennas under the following illustrative
conditions. First, for a ULF receiver at a
100 m depth in the sea and a VMD (horizontal
loop antenna) at an altitude of 3000 m above
the sea, air/undersea communication at 1 Hz
is possible for horizontal distances in the
range 0 to 10 km for a VMD moment of 10^7 A m^2
or in the range 0 to 33 km for a VMD moment
of 10^7 A m^2

Second, for an HMD (vertical loop antenna)
at an altitude of 3000 m and a ULF receiver
located at a depth of 100 m directly ahead
or behind of the HMD, air/undersea communi-
cation at 1 Hz is possible for horizontal

65

distances in the range 0 to 13 km for an
HMD moment of 10^7 A m^2 or in the range
0 to 64 km for an HMD moment of 10^9 A m^2.
Note that the maximum distance of communi-
cation for a VMD can be increased (a) by
increasing the height of the dipole (within
a limit set by the size of the dipole
moment) and (b) by reducing the depth of the
ULF receiver, whereas at a given azimuthal
angle the maximum distance of communication
for an HMD can only generally by increased
by reducing the depth of the ULF receiver.

(iv) For both the VMD and the HMD it is possible
to limit air/undersea communication at 1 Hz
to a comparatively small circular area
directly beneath the dipole source. The
radius of this circular area can be adjusted
within wide limits by varying (a) the dipole
moment and (b) the altitude of the dipole,
and it can be as small as 400 m for a 10^3 A m^2
VMD at an altitude of 300 m (for a ULF
receiver at any depth in the range 0 m to
200 m).

For the VMD, it is also possible to limit
air/undersea communication at 1 Hz to an
annular area centered on the point directly

66

below the dipole source. In this case a
circular "dead" area is produced directly
below the dipole where the magnetic field
is too weak to be measured. The conditions
for producing the limited annular area re-
quire dipole altitudes in the approximate
range 1 km to 10 km and, for a given dipole
altitude, involve a highly restricted range
of dipole moments. Because of these re-
strictions, this mode of air/undersea com-
munication is considered less likely to have
a practical use than the mode involving com-
munication to a limited circular area directly
beneath the dipole.

(v)   The maximum range for air/undersea communi-
cation at 1 Hz is smaller for a VMD than it
is for an HMD of the same moment. However,
the VMD total magnetic field does not have
either (a) an azimuthal angle dependence or
(b) field geometry minimums. In a situation
where range is not a primary consideration,
the more regular behaviour of the VMD field
may give the VMD an advantage over the HMD
for air/undersea communication.

67

(vi)   For ULF receivers on or close to a sea floor
         of low electrical conductivity ($\sigma \leq 10^{-2}$ mho/m),
         our calculations indicate that the total
         magnetic field produced by an airborne loop
         antenna at horizontal distances greater than
         about 10 km can be increased or decreased by
         up to an order of magnitude by the presence
         of the sea floor (compared with the total
         magnetic field that would be produced at the
         same points in an infinitely deep sea). We
         therefore believe that sea floor effects
         require further study.

(vii)   Changes in the impedance of airborne loop
         antennas caused by the proximity of the
         antennas to the sea water are likely to be
         completely negligible.

Throughout this report we have used 1 Hz as a representative ULF
frequency. Consideration of the natural ULF noise background, the low
data rate at 1 Hz; and the low attenuation of 1 to 6 Hz electromagnetic
fields in a 200 m maximum depth of sea water lead us to the following
conclusion:

(viii)   The more favorable ULF frequencies for air/
         undersea communication lie in the range 1 to
         6 Hz.

68

Finally, in summary, we conclude:

(ix) Airborne loop antennas operating at frequencies
in the ULF range and with maximum moments in the
range 10^7 A m^2 to 10^9 A m^2 offer a feasible means
of transmitting command and control messages
(i.e., short standardized messages of high in-
formation content) to submerged ULF receivers at
depths in the range 0 to 200 m and at horizontal
distances in the approximate range 0 to 60 km.
Possible improvement in the sensitivity of the
submerged ULF receivers, particularly submerged
ULF receivers in motion, and the provision of
greater power for the loop antennas could con-
ceivably increase the maximum horizontal range
to about 100 km.
In a situation where secure communication is
a primary requirement (and not maximum hor-
izontal range), ULF communications from an
airborne loop antenna can be limited to sub-
merged ULF receivers in a restricted area
directly beneath the loop antenna. The size
this area can be controlled within wide
limits by variation of the altitude and
moment of the loop antenna.

69

5. Recommendations

The preceding conclusions are based largely on the results of our calculations of the 1 Hz total magnetic field produced in the sea by airborne loop antennas and on information that is sometimes incomplete or not in an entirely suitable form for use in the present study. Further progress in air/undersea communication at ULF will require additional field calculations and new information as suggested in the following recommendations.

(i) Design of a compact, lightweight, superconducting current loop with a high magnetic moment ($m \geq 10^9$ A m^2) that can be switched or alternated at frequencies in the ULF range would represent a major advance for air/undersea communication at ULF. Further studies of high-moment superconducting current loops is strongly recommended.

(ii) Continued development of highly-sensitive towed total field magnetometers, particularly for use at ULF, would complement the effort to develop an airborne loop antenna of high magnetic moment.

(iii) Measurements of the ULF background magnetic
noise in the sea at different depths (in the
range 0 to 200 m) for various sea states and
for different levels of natural geomagnetic
activity are desirable. Measurements both
on and above the sea floor are needed, as well
as measurements in a very deep sea (no sea
floor effect).

(iv) The research recommended in (iii) would be
strengthened by a parallel theoretical effort
to derive spectrums of the ULF/ELF electro-
magnetic fields generated at different depths
in the sea for representative sea states.

(v) Additional calculations of the effects pro-
duced by a realistic sea floor on the ULF
fields generated in the sea by elevated
dipole sources would help establish the
importance of a sea floor in air/undersea
communication.

71

REFERENCES

Arnold, H. A., "Manned submersibles for research," _Science_, 158, 84, 1967.

Baños, A., Jr., _Dipole Radiation in the Presence of a Conducting Half-Space_, Pergamon Press, New York, 1966.

Bernstein, S. L., M. L. Burrows, J. E. Evans, A. S. Griffiths, D. A. McNeill, C. W. Niessen, I. Richer, D. P. White, D. K. Willim, "Long-range communications at extremely low frequencies," _Proc. IEEE_, 62, 292, 1974.

Bubenik, D. M., "A practical method for the numerical evaluation of Sommerfeld integrals." To appear in _IEEE Trans. Ant. Prop._, 1977.

Burrows, M. L., "The Lincoln submarine towed ELF loop antenna," Tech. Note 1975-24, M.I.T. Lincoln Lab., Lexington, MA, 27 May 1975.

Buxton, J. L., and A. C. Fraser-Smith, "A superconducting system for high sensitivity measurements of Pc 1 geomagnetic pulsations," _IEEE Trans. Geosci. Elec._, GE-12, 109, 1974.

Davis, J. R., J. W. Willis, and E. L. Althouse, "Magic mode. Investigations of artificial stimulation of ULF waves in the ionosphere and magnetosphere," _Naval Res. Lab._, _Rept. 7552_, March 1973.

Davis, J. R., and J. W. Willis, "A quest for a controllable ULF wave source," _IEEE Trans. Commun._, COM-22, 578, 1974.

Davis, J. R., R. J. Dinger, and J. A. Goldstein, "Development of a superconducting ELF receiving antenna," _IEEE Trans. Ant. Prop._, AP-25, 223, 1977.

Durrani, S. H., "Air-to-undersea communication with electric dipoles," _IRE Trans. Ant. Prop._, 10, 524, 1962.

Durrani, S. H., "Air to undersea communication with magnetic dipoles," _IEEE Trans. Ant. Prop._, 12, 464, 1964.

Fraser-Smith, A. C., "Chevron frequency structure in Pc 1 geomagnetic pulsations," _Geophys. Res. Letts._, 4, 53, 1977.

Fraser-Smith, A. C., K. J. Harker, R. T. Bly, Jr., and D. M. Bubenik, "Generation of artificial geomagnetic micropulsations with a large ground-based current loop," _Stanford Elec. Lab. Rept. SU-SEL-72-023_, Contract N00014-67-A-0112-0066, Stanford University, Stanford, CA, June 1972.
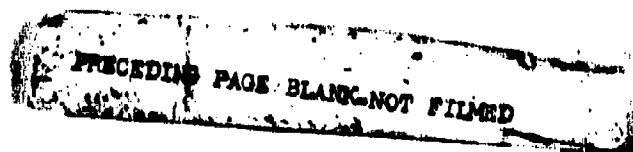
Fraser-Smith, A. C., and J. L. Buxton, "Superconducting magnetometer measurements of geomagnetic activity in the 0.1 to 14 Hz frequency range," J. Geophys. Res., 80, 3141, 1975.

Fraser-Smith, A. C., and D. M. Bubenik, "ULF/ELF magnetic fields generated at the sea surface by submerged magnetic dipoles," Radio Sci., 11, 901, 1976.

Golub, G. H., and J. H. Welsch, "Calculation of Gaussian quadrature rules," Math. Comp., 23, 221, 1969.

Greifinger, C., "Feasibility of ground-based generation of artificial micropulsations," J. Geophys. Res., 77, 6761, 1972.

Greifinger, C., and P. Greifinger, "Generation of ULF by a horizontal electric dipole," Radio Sci., 9, 533, 1974.

Harker, K. J., "Generation of ULF waves by electric or magnetic dipoles," J. Geophys. Res., 80, 3100, 1975.

Heirtzler, J. R., and J. F. Grassle, "Deep-sea research by manned submersibles," Science, 194, 294, 1976.

ITT, Reference Data for Radio Engineers, 5th Edition, published by International Telephone and Telegraph Corp., New York, 1968.

Jacobs, J. A., Geomagnetic Micropulsations, 179 pp., Springer, New York, 1970.

Kermabon, A., C. Gehin, and P. Blavier, "A deep-sea electrical resistivity probe for measuring porosity and density of unconsolidated sediments," Geophysics, 34, 554, 1969.

Kirkpatrick, R. J., "Results of downhole geophysical logging; Hole 396 B, DSDP Leg 46 (Glomar Challenger)," Preprint, Scripps Institute of Oceanography, La Jolla, CA, 1977.

Kraichman, M. B., Handbook of Electromagnetic Propagation in Conducting Media, 124 pp., U.S. Government Printing Office, Washington, D.C., 1970.

Maclure, K. C., R. A. Hafer, J. T. Weaver, "Magnetic variations produced by ocean swell," Nature, 204, 1290, 1964.

Morrison, H. F., and W. M. Dolan, "Earth conductivity determination employing a single superconducting coil," Geophysics, 38, 1214, 1973.

Podney, W., "Electromagnetic fields generated by ocean waves," J. Geophys. Res., 80, 2977, 1975.

Ryu, J., H. F. Morrison, and S. H. Ward, "Electromagnetic fields about a loop source of current," Geophys., 35, 862, 1970.

Scoville, H., "Missile submarines and national security," <u>Sci. Am.</u>, <u>226</u> (6), 15, 1972.

Shanks, D., "Non-linear transformations of divergent and slowly convergent sequences," <u>J. Math. Phys.</u>, <u>34</u>, 1, 1955.

Sommerfeld, A., "Über die Ausbreitung der Wellen in der drahtlosen Telegraphie," <u>Ann. Phys.</u>, <u>28</u>, 665, 1909.

Wait, J. R., "Theory of ground wave propagation," in <u>Electromagnetic Probing in Geophysics</u>, p. 163-207, Ed. J. R. Wait, Golem Press, Boulder, CO, 1971.

Wait, J. R., "Project Sanguine," <u>Science</u>, <u>178</u>, 272, 1972.

Wait, J. R., and K. P. Spies, "Low-frequency impedance of a circular loop over a conducting ground," <u>Electron. Letters</u>, <u>9</u>, 346, 1973.

Warburton, F., and R. Caminiti, "The induced magnetic field of sea waves," <u>J. Geophys. Res.</u>, <u>69</u>, 4311, 1964.

Wolf, S. A., J. R. Davis, and M. Nisenoff, "Superconducting extremely low frequency (ELF) magnetic field sensors for submarine communications," <u>IEEE Trans. Commun.</u>, <u>COM-22</u>, 549, 1974.

DISTRIBUTION LIST

Organization	No. of Copies	Organization	No. of Copies

Director
Defense Advanced Research
  Projects Agency
ATTN: Program Management
1400 Wilson Boulevard
Arlington, VA 22209
	2	Naval Ocean Systems Center
		ATTN: Library
		        V. Hildebrand Code 812
		271 Catalina Boulevard
		San Diego, CA 92152
			1
			1

Defense Documentation Center Cameron Station Alexandria, VA 22314	12	Naval Electronics Systems Command ATTN: PME-117 Department of Navy Washington, D.C. 20360	1

Office of Naval Research
ATTN: Code 1021P
        Code 461FP
800 N. Quincy St.
Arlington, VA 22217
	6
	2
		Naval Underwater Systems Center
		New London Laboratory
		ATTN: P. Bannister
		        A. Bruno
		        J. Orr
		        E. Soderberg
		New London, CT 06320
			1
			1
			1
			1

Office of Naval Research
Resident Representative
University of California
  San Diego
La Jolla, CA 92093
	1	Naval Surface Weapons Center
		White Oak Laboratory
		ATTN: M. B. Kraichman
		        P. Wessel
		Silver Spring, MD 20910
			1
			1

Office of Naval Research Resident Representative Stanford University Room 165 - Durand Building Stanford, CA 94305	1	Director Defense Nuclear Agency Washington, D.C. 20305	1
Chief of Naval Operations OASN (R&D), Rm. 4E 741 ATTN: T. P. Quinn Pentagon Washington, D.C. 20350	1	R & D Associates ATTN: C. Greifinger P. O. Box 9695 Marina del Rey, CA 90291	1
Naval Research Laboratory ATTN: Code 2627 J. R. Davis 4555 Overlook Avenue, SW Washington, D.C. 20375	6 1	Pacific-Sierra Research Corp. ATTN: E. C. Field 1456 Cloverfield Blvd. Santa Monica, CA 90404	1